IEEE Access
Multidisciplinary | Rapid Review | Open Access Journal

Received March 14, 2022, accepted March 29, 2022, date of publication April 7, 2022, date of current version April 15, 2022.

Digital Object Identifier 10.1109/ACCESS.2022.3165574

Skin Disease Analysis With Limited Data in Particular Rosacea: A Review and Recommended Framework

ANWESHA MOHANTY, (Graduate Student Member, IEEE), ALISTAIR SUTHERLAND, MARIJA BEZBRADICA, AND HOSSEIN JAVIDNIA
School of Computing, Dublin City University, Dublin 9, D09 V209 Ireland

Corresponding author: Anwesha Mohanty (anwesha.mohanty2@mail.dcu.ie)

This work was supported by the Science Foundation Ireland Centre for Research Training in Digitally-Enhanced Reality (d-real) under Grant 18/CRT/6224.

ABSTRACT Recently, the rapid advancements in Deep Learning and Computer Vision technologies have introduced a new and exciting era in the field of skin disease analysis. However, there are certain challenges in the roadmap towards developing such technologies for real-life applications that must be investigated. This study considers one of the key challenges in data acquisition and computation, viz. data scarcity. Data scarcity is a central problem in acquiring medical images and applying machine learning techniques to train Convolutional Neural Networks for disease diagnosis. The main objective of this study is to explore the possible methods to deal with the data scarcity problem and to improve diagnosis with small datasets. The challenges in data acquisition for a few lamentably neglected skin conditions such as rosacea are an excellent instance to explore the possibilities of improving computer-aided skin disease diagnosis. With data scarcity in mind, the possible techniques explored and discussed include Generative Adversarial Networks, Meta-Learning, Few-Shot classification, and 3D face modelling. Furthermore, the existing studies are discussed based on skin conditions considered, data volume and implementation choices. Some future research directions are recommended.

INDEX TERMS Artificial intelligence, dermatology, generative adversarial networks, image analysis, meta-learning, neural network, rosacea, skin disease diagnosis, teledermatology.

I. INTRODUCTION

Skin is the largest organ of the human body which plays an important role in protecting the body from harsh chemical and environmental conditions. Skin diseases affect one third of the world's population [1]. According to a report published by the National Centre for Biotechnology Information (NCBI) in 2017, skin diseases are the fourth leading cause of non-fatal diseases worldwide [2]. Skin diseases cause discomfort in day-to-day life. They get worse with time, reduce productivity in the daily regime and, if not treated at the early stage, can be deadly. Skin diseases are not only a problem for individuals but for the world population posing an increasing economic threat to national healthcare systems worldwide [3]. According to one of the latest survey report published in 2013 by European Dermatology Health Care, the 10 countries with longest waiting times for regular dermatological visits from 40 days to 133 days are: Germany, Malta, Austria, Luxembourg, Sweden, Poland, Norway, UK, Slovenia and Ireland [4]. Likewise, there are only a few dermatologists per 100,000 population in many countries. Table 1 highlights the limited number of dermatologists in six different countries gathered from the official sources. Given the low number of dermatologists and long waiting times, it is essential to expand the scope of skin treatment through computer-aided diagnosis.

To complement the work of qualified dermatologists, skin disease diagnosis using Computer Vision and Machine Learning is important in contributing to the early diagnosis process performed by healthcare professionals such as General Practitioners and Dermatologists. From the early 90s, dermatologists have been collectively working via digital platforms to communicate and diagnose skin diseases of patients by utilising skin disease images and additional health

The associate editor coordinating the review of this manuscript and approving it for publication was Yizhang Jiang.

TABLE 1. Number of dermatologists in six different countries.

Country	No. of Dermatologists per 100,000 population	Source
United Kingdom	1.4	British Association of Dermatology, 2013 [5]
Ireland	1	Health Service Executive (HSE), Ireland, 2014 [6]
Canada	0.47 (rural) 1.96 (urban)	Royal College of Physicians and Surgeons of Canada, 2019 [7]
USA	3.4	Journal of American Medical Association (JAMA), American Academy of Dermatology (AAD), 2016 [8]
Australia	1.9	Australian Government, Department of Health, 2016 [9]
China	1	Chinese Medical Journal, 2019 [10]

data. In medical literature, this technique of collecting, monitoring, storing, and sharing data in order to help diagnose skin conditions is termed ''Teledermatology'' [11].

There are various ways of diagnosing skin diseases through imaging. The three most common kinds of skin image data are: histopathological, dermoscopic, and clinical images. A few existing studies on skin disease diagnosis using traditional machine learning algorithms have been done using histopathological images for cancerous skin conditions. Most of the work on skin diseases has been done using dermoscopic images, primarily cancerous skin lesions. However, only a few studies have been done on clinical images of common and chronic skin conditions such as acne, rosacea, eczema, lupus, seborrheic dermatitis, and a few other conditions. Hence, there is a need for attention to these diseases in medical image analysis using advanced machine learning and computer vision techniques. However, there are specific challenges to be dealt with due to the nature of these diseases and the availability of datasets. For example, a specific skin condition called rosacea will be looked at in this review. In the case of rosacea (as for the other conditions), there is only a limited amount of image data available. In this review, we explore the following approaches to dealing with limited data.

1) Data Augmentation, i.e. generating synthetic data with slight modifications to complement the real data.
2) Transfer learning and fine-tuning i.e. adapting a neural network model, which has been pre-trained on another much larger dataset, to classify rosacea.
3) Generative Adversarial Networks (GANs) i.e. generating high quality synthetic faces with rosacea.
4) Meta-Learning and Few-Shot classification i.e. learning faster with fewer examples.
5) 3D Morphable Face Models i.e. creating a 3D model of human face with various subtypes of rosacea from a set of 2D images.

In this literature review, we are investigating skin diseases, especially the importance of rosacea diagnosis using machine learning and computer vision. In Section I.A., skin diseases, types of medical diagnosis, types of images used in computer vision and machine learning tasks for diagnosis of skin conditions are discussed. In Section I.B., the motivation for rosacea image analysis is discussed. Section II is focused on a few existing studies carried out on rosacea using machine learning and computer vision. In Section III, we discuss how the amalgamation of big data, deep learning and computer vision has brought some breakthroughs in the field of medical diagnosis. This discussion is followed by the challenges of having a smaller dataset in the field of medical diagnosis and how to leverage a smaller dataset using various techniques of machine learning and computer vision. Hence, in section IV, we discussed various publicly available datasets.

Section V provides a brief overview of skin disease analysis from traditional machine learning and computer vision techniques to the modern deep learning algorithms. Section V contains four subsections in which four techniques in machine learning and computer vision are discussed, a few existing studies using Data Augmentation and Transfer Learning in Section V.A, Generative Adversarial Networks in Section V.B, Meta-Learning and Few-Shot Classification in Section V.C, 3D Face Modelling in Section V.D. The challenges and major takeaways are mentioned in each sub section of these four techniques. Furthermore, based on a few key points from the literature review, the implementation possibilities of GANs, Meta-learning, and 3D Face Modelling in the limited data scenario are discussed in Section VI. Based on the options for implementation, some future directions are recommended.

A. A BRIEF INTRODUCTION TO SKIN DISEASES

Skin diseases are one of the most challenging fields in medical diagnosis due to their observational and analytical complexities. Diagnosis of skin diseases requires years of experience and expertise. Skin diseases are diagnosed visually, with an initial screening followed by dermoscopic analysis, biopsy and histopathological analysis. However, this process of diagnosis is time-consuming and costly. Chronic inflammatory skin diseases which may not be fatal in most situations, may still need lifelong engagement with dermatologists. Chronic skin conditions need regular check-ups, up to date medications, surgical or laser treatments, if required. This way of treatment requires a significant amount of time and are often costly. However, detecting chronic skin conditions at the early stages allows for an intervention and prevention of further complications. Several technically advanced hospitals in the world follow a dynamic process for treating skin diseases. This requires patient record-keeping, including images of the skin diseases and basic information about the patients, which helps monitor the progress of the treatment over time.

One of the traditional and common techniques to collect patient data for diagnosing skin diseases is dermoscopic imaging. Dermoscopic images are collected through high quality magnifying lenses (mainly through a dermatoscope)

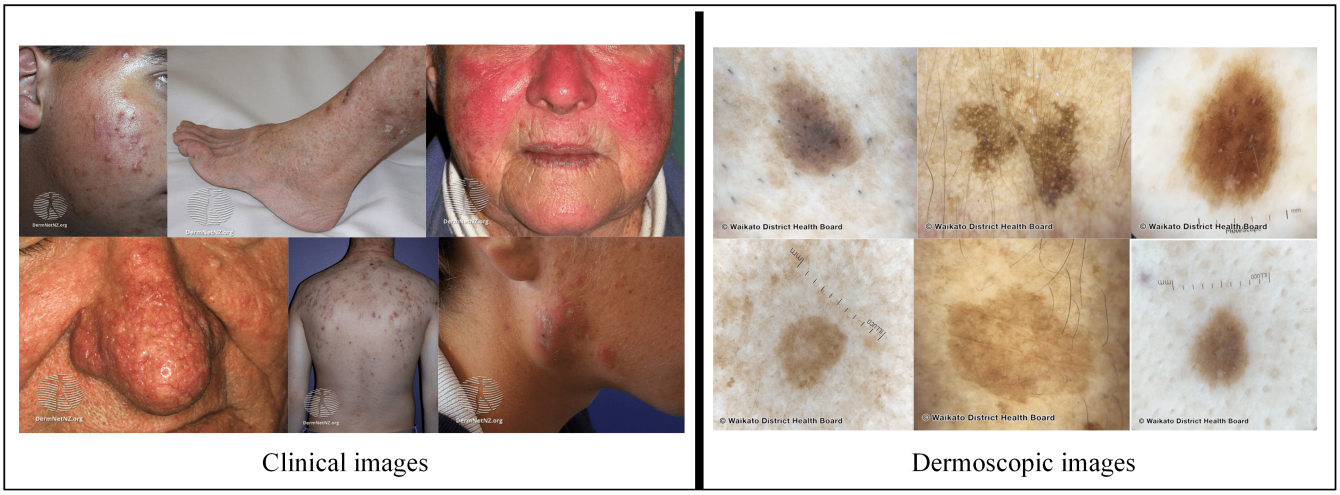

FIGURE 1. **Clinical images vs. Dermoscopic images. The images used in this figure are taken from DermnetNZ [13].**

with powerful lighting. The most common types of images captured by the dermatoscopes are micro and macro images of individual lesions which lose the anatomical details of the body. Further, these dermoscopic images are captured and examined by specialist dermatologists. Hence, dermoscopic images are very useful when diagnosing individual skin lesions such as malignant and benign lesions on the body. However, it is not possible to capture dermoscopic images for every skin condition at the initial stage of the disease. For this purpose, using a good quality digital camera or smartphone can facilitate capturing images of common skin diseases making smart phones or other digital photographic devices an accessible alternative for capturing skin conditions at the early stage of the diagnosis. The skin images captured by smartphone or other photographic devices are referred to as ''clinical'' images in the world of medical science research. As a result, clinical images are gaining popularity in skin disease diagnosis [12] and there are many medical research platforms that encourage collecting clinical images. Fig. 1, illustrates a few samples of clinical and dermoscopic images.

1) MOTIVATION FOR ROSACEA IMAGE ANALYSIS

Rosacea is a chronic facial skin condition that goes through a cycle of fading and relapse [14]. It is also a cutaneous vascular disorder [15]. It is a common skin condition in native people from northern countries with fair skin or Celtic origins [16]. Rosacea is often characterized by signs of facial flushing and redness, inflammatory papules and pustules, telangiectasias, and facial edema. Rosacea's symptom severity varies greatly among individuals [17]. In the medical diagnostic approach, rosacea is classified into four subtypes – Subtype 1 (Erythematotelangiectatic rosacea), Subtype 2 (Papulopustular rosacea), Subtype 3 (Phymatous rosacea) and Subtype 4 (Ocular rosacea). Each subtype is diagnosed based on the severity of condition e.g. mild, moderate, or severe [14], [18].

According to an article published by the National Rosacea Society (NRS) (United States) in 2018, there are nearly 415 million people affected by rosacea worldwide [19]. This condition has a higher incidence in women than men, although it tends to be more severe in men [16]. Rosacea is often an underdiagnosed condition. Given the fact rosacea is often characterized by signs of facial redness and flushing, this leads to frequent misdiagnosis as seborrheic dermatitis, although seborrheic dermatitis and rosacea are unrelated [20]. Rosacea is also frequently mistaken as psoriasis, lupus, acne, and eczema [20].

Besides the clinical complications, rosacea can affect patients' overall wellbeing, social life and work life. According to a survey carried out by National Rosacea Society of Canada, among 700 patients with rosacea in the working group, 66% were affected in their professional interactions, 33% had cancelled or postponed business meetings, 28% had missed work, 28% felt rosacea may have negatively influenced their chances of a promotion. In another survey with 660 patients with severe cases of rosacea, 86% of participants reported that they had to limit their social lives due to rosacea [21].

'British Association of Dermatologists' reported that rosacea is a facial dermatosis and therefore easily visible. It can cause extreme discomfort to those who suffer from it [18]. According to another study conducted by Spoendlin *et al.* [22] based on data collected in the period of 1995-2009, rosacea was diagnosed in 80% of cases after the age of 30 years, in which 61.5% patients were women.

According to the 'Acne and Rosacea Society of Canada' more than 3 million Canadians suffer from rosacea [23]. It is anticipated to become one of the most common health problems in Canada. One study in Sweden found that women with rosacea are more likely to experience migraine headaches than those with healthy skin conditions [24]. In 2019, according to a Market Analysis Report published by Grand View Research [25], the rosacea treatment market will be worth $2.6 billion by 2025, proving one of the fastest growing drug classes. In April 2021, a report published by the National

Rosacea Society [26], states, ''New treatments continue to expand therapy options, but a cure remains elusive''. The reasons behind the continued growth of rosacea cases in recent years are: lack of awareness in dermatologists, misdiagnosis, cost of treatment etc. [26].

In a recent article published by US News Health, ''rosacea is often misdiagnosed, and many don't seek treatment because they don't realize it's rosacea,'' says Jeffrey Fromowitz, MD, FAAD, a dermatologist based in Boca Raton, Florida [27]. Frequent news on rosacea awareness and treatment appears regularly in the Irish times [28], Irish Examiner, and a few other newspaper organisations in Ireland. This indicates the global scale of the problem of rosacea. As the concern rises, the treatment of rosacea is not only the responsibility of expert dermatologists, but Machine Learning can also be a potential pathway towards the early diagnosis of rosacea with state-of-the-art methodologies. A fast, accurate and low-cost assistive diagnostic system could significantly contribute to medical treatment plans, particularly in developing countries. Early and accurate detection of skin lesions, inflammation and facial skin conditions, such as rosacea, is vital for developing precise and effective treatment and medication. In this review we provide a critical literature review and an analysis on skin disease diagnosis using various methodologies of machine learning and computer vision.

II. RELATED WORK ON ROSACEA

In recent years, medical image diagnosis has progressed rapidly due to the advancement of Artificial Intelligence (AI) models and the availability of a large amount of data provided by medical professionals. Thanks to the advanced machine learning and deep learning techniques in computer vision, different types of disease diagnosis have become very widespread in the scientific and medical research community. An extensive amount of work has been done on skin cancer diagnosis. According to a study published by Stanford University in 2017 [29], Dermatological (dermoscopic) images play an important role in diagnosing skin cancer using Deep Convolutional Neural Networks (DCNNs) [30]. The work by Esteva *et al.* [29]suggests that the diagnosis technique could be used outside the clinic as an initial screening step for cancer to a level of competence comparable to 21 board-certified dermatologists. Since then, computer vision and deep learning research has attracted a lot of attention for skin cancer lesion classifications by proposing various kinds of state-of-the-art methodologies and techniques. However, most of the work on skin disease analysis and classification so far has been done is on dermoscopic images, in which a particular region of interest of the skin is focused on, as shown in Fig. 1; while there are very few studies on facial skin conditions such as rosacea, rosacea acne, eczema, psoriasis lupin and other related skin conditions. Table 2 presents an overview of studies conducted on rosacea along with other skin conditions.

As it can be seen from Table 2, most of the studies which have been carried out on rosacea and related skin conditions using machine learning and computer vision/deep learning algorithms date from the year 2019 and onwards. Most of the works which have shown great results using deep learning have used at least nearly 10,000 images. A few studies conducted by Thomsen *et al.* [31], Zhao *et al.* [32], Wu *et al.* [33] and Zhu *et al.* [34], employ a significant quantity of data. However, the datasets used in these studies are entirely confidential. Hence these studies are not entirely reproducible and therefore there is a motivation for other researchers to try to deal with the skin disease problem using limited data. Most of the work done so far using transfer learning and data augmentation has used weights pre-trained on ImageNet [35], which is considered a non-medical dataset. However, these studies provide a useful insight into a few common techniques which can be applied in this research. A few studies have shared their GitHub repository, which may provide references for publicly available datasets.

Goceri [36] presented a novel modified Mobile-Net architecture [37] along with a mobile app with user-friendly interface. In this work, 725 images of seborrheic dermatitis, rosacea, hemangioma, psoriasis and acne vulgaris were used for classification tasks. There were 145 images in each disease class. The modified Mobile-Net model was developed based on the original Mobile-Net architecture but with the receptive field expanded, with dilated convolution and combined hybrid loss functions.The experimental results in this study have shown that the proposed modified Mobile-Net [36] has outperformed other network architectures for each disease class.

Thomsen *et al.* [31] presented a dataset and a classification task with 5 categories of skin conditions i.e. Psoriasis, Eczema, cutaneous t-cell lymphoma, acne and rosacea. As part of the pre-processing before the classification task, K-means clustering was used to remove the noise and unnecessary details from the images. There were 4 types of modified VGG-16 [38] CNN architectures with and without Spatial Transformer Network (STN) are listed in the Table2. According to the results discussed in this study, these 4 types of VGG-16 architecture performed differently in terms of Area Under the Curve (AUC) and accuracy scores for each disease class. However, VGG-16P is proven to be the best performing model after the performance measured through specificity, sensitivity, Positive Predictive Value (PPV), and Negative Predictive Value (NPV). Additionally, the overfitting due to the small datasets and selection bias for acne and rosacea is an issue and was discussed in this study.

Goceri [39] proposed a segmentation method called Fully Automated Detection of Facial Disorders (F-ADFD). This method has shown better segmentation accuracy, specificity, and precision due to active contouring which is set automatically using a binary image that is obtained with a K-means clustering after denoising and intensity normalization steps. Among 10 Deep Neural Net (DNN) architectures that were used in this work, DenseNet201 [40] with modified loss function (cross-entropy and Tversky similarity) was claimed to have shown results with maximum accuracy (95.24%) and

minimum loss (0.5). The second highest performance was obtained by InceptionResNet-v2 [41]. This study suggests that DNN techniques can extract features automatically at low, middle and, high levels by increasing depth and by performing classification for skin lesions. All the DNN architectures used in this work were pretrained on ImageNet [35].

Zhao *et al.* [32] carried out a study on three subtypes of rosacea lesions i.e. Erythematotelangiectatic rosacea (ETR), papulopustular rosacea (PPR), and phymatous rosacea (PhR). The accuracy of the CNN to classify one subtype against the others was 83.9%, 74.3%, and 80.0% for ETR, PPR, and PhR, respectively. This work also included other types of skin conditions such as acne, facial eczema and seborrheic dermatitis, lupus erythematosus, chronic solar dermatitis, corticosteroid-dependent dermatitis, lupus miliaris disseminatus faciei; which may look like rosacea. A total of 24,736 images were used in this study. However, there is no information provided regarding the source of the dataset and the dataset used to obtain the results is not publicly available. This study also discussed the need for exploring the ways of decision-making in deep CNNs, which may help in improving the accuracy and specificity for the detection of diseases.

Wu *et al.* [33] performed a classification among psoriasis (Pso), eczema (Ecz), Atopic dermatitis (AD) and Healthy skin. This work did not use any rosacea images, and instead relies on hand and facial images. The study involved 4,740 images collected from the Department of Dermatology, The Second Xiangya Hospital, Central South University, China. However, this dataset is confidential. Google's EfficientNet-b4 [42] was used with an extra 7 auxiliary classifiers at the end of each intermediate layer to make the model learn classification information from different levels of features. This work was built as a smart phone mobile application.

Zhu *et al.* [34] performed a classification among 14 skin diseases with 13,603 images labeled by two dermatologists with a minimum of 5 years of experience. This data was collected from the Department of Dermatology, Peking Union Medical College Hospital, China, from April 2016 to April 2020. In this work, EfficientNet-b4 [42] was used with pre-trained weights from ImageNet. There were 14 classifiers with 14 output neurons used instead of the final fully connected classification layer of the network. This modified model of EfficientNet-b4 is compared with Inception-v3 [43], ResNet-101 [44] and the original EfficientNet-b4 [42]. The comparative outcomes are measured by AUC, ROC, Sensitivity, Specificity and Accuracy. The modified EfficientNet-b4 has outperformed other CNN models with an AUC of 0.985 and with the highest ROC. The performance of modified(proposed) EfficientNet-b4 was also compared with dermatologists, in which performance is measured using the Kappa coefficient. This performance measure comparison showed that the diagnosis of Rosacea by dermatologists is significantly better than the proposed model. In comparison, the diagnosis of viral warts by the proposed model was significantly better than the dermatologists.

Aggarwal [45] looked at 5 skin conditions: acne, atopic dermatitis, impetigo, psoriasis, and rosacea. A total of 938 images were considered for classification using Inception-v3 with pre-trained weights of ImageNet [35]. Data Augmentation was incorporated during the training process to reduce the possibility of overfitting. The performance of the model was measured through sensitivity, specificity, positive predictive value (PPV), negative predictive value (NPV), Mathew's correlation coefficient (MCC), and F1 score. A comparative result illustrated how each model performed with and without data augmentation. From the confusion matrix, the performance scores for rosacea are relatively low (0.60 with data augmentation) compared to the other four skin conditions. The number of images of rosacea considered in this study was 90.

Binol *et al.* [46] presented a study using rosacea images collected from the Division of Dermatology at Ohio State University. There were 41 images collected using a DSLR camera, in which images were taken from left, right, front and upsides of the faces. There were two CNN models considered for classification i.e. Inception-ResNet-v2 [41] and ResNet-101 [44] with the pre-trained weights from ImageNet [35]. A few pre-processing tasks were performed, such as creating labelled patches on the facial images. These patches were labelled by expert dermatologists based on the anatomical details of the face. The anatomical parts of the face regions more than 75% affected by rosacea were labelled as positive rosacea patches and less than 25% rosacea affected regions were labelled as negative rosacea patches. The patches with various resolutions such as 64×64, 128×128, 256×256 were obtained for the data augmentation and transfer learning process. Hence there were nearly 65,649 tiles with different resolutions crafted on the 41 images. The accuracy of the models was measured using Dice Coefficient and false-positive rate. A specific kind of post-processing was proposed in this work called Anthropometric Post-Processing (APP) with a landmarks-based Region of Interest (ROI) mask. The Inception-ResNet-v2 [41] with APP provided a higher performance score compared to other models such as ResNet101 [44] and Bag of Features with Support Vector Machine (SVM).

Xie *et al.* [47] presented a dataset and classification task for 541 skin conditions. The image dataset was collected using 4 types of digital cameras, and these images were annotated by 20 professional dermatologists from the Xiangya Hospital of Central South University, China. However, in this study, 80 categories of skin conditions were considered for classification. The disease categories considered had more than 100 images and the categories with more than 1000 images were discarded to keep a balance during the classification process. There were 4 types of CNN architectures considered for the task i.e. InceptionResNet-v2 [41], Inception-v3 [43], Densenet121 [40] and Xception [48]. According to the results drawn from the confusion matrix, InceptionResNet-v2 outperformed the other three CNN architectures with 0.764 accuracy.

III. LEARNING - FROM "Big DATA" TO "Small DATA"

The concept of visual data – 'image datasets' started gaining popularity in 1999 through the release of an official standard database i.e. the MNIST database (Modified National Institute of Standards and Technology database) by Yann Le Cun and his colleagues [49], [50]. The MNIST database is a collection of handwritten digits. It has a training set of 60,000 example images and a test set of 10,000 images.

In 2009, Deng *et al.* [35] introduced ImageNet, one of the largest image datasets available containing around 3.2 million images. Based on the numbers recorded on the ImageNet homepage, there are more than 14 million images in the dataset with just over 21 thousand synsets (groups/classes).

The real-world artefacts which humans can recognise have now become recognisable by computers through efficient algorithms and large sets of images, which was a difficult task a decade earlier. These advancements have become possible due to the availability of large volume datasets like ImageNet [35], which can be fundamentally called 'Big Data'. Having bigger datasets is one of the key prerequisites for Deep Learning models to perform well.

A. BIG DATA IN COMPUTER-AIDED MEDICAL DIAGNOSIS

Medical image analysis using deep learning has become popular among research communities due to the collective concept of 'Big Data'. According to the studies reviewed in this work, the volume of the data used for medical diagnosis is three to four times smaller than the number of images in ImageNet [35].

One of the influential works by Esteva *et al.* [29] on skin disease analysis with dermoscopic images for diagnosing skin cancer created a new trend for skin disease analysis using deep learning and computer vision. In total 129,450 clinical images were used in [29] to train a deep convolutional neural network to classify the most common deadliest skin cancer. Advances in medical image analysis techniques have also been used for other conditions. For instance, Ting *et al.* [51] utilised a dataset of 494,661 retinal images to diagnose Diabetic Retinopathy and related eye diseases from visual scans. In order to detect bone fractures in radiographs, a deep learning model trained on 135,845 radiographs of a variety of body parts was proposed with a diagnostic accuracy similar to that of senior subspecialized orthopedic surgeons [52]. This work claims that, given enough training data and a suitably designed model, it is possible to detect any condition on radiographs that a human clinician could identify. A deep learning model, DeepSeeNet [53] was developed to classify patients with Age-related Macular Degeneration (AMD). DeepSeeNet was trained on 58,402 training images and 900 testing images collected from 4549 participants. In another attempt, a deep learning model was trained for automatic Magnetic Resonance Imaging (MRI) cardiac multi-structure segmentation and diagnosis [54]. It used the "Automatic Cardiac Diagnosis Challenge" dataset (ACDC), the largest publicly available and fully annotated dataset for Cardiac MRI (CMRI) assessment. The dataset contains CMRI recordings obtained from 150 devices, with reference measurements and classification from two medical experts.

B. IMPORTANCE OF THE 'small DATASETS' IN MEDICAL DIAGNOSIS

Although deep learning models have exhibited prodigious performance in computer vision tasks such as automated diagnosis of medical conditions (diabetes, retinopathy, bone fractures, age-related macular degeneration, cardiac MRI and skin cancer, etc.), they heavily rely on a large volume of the labelled dataset [55]. While these models are helping to achieve breakthrough state-of-the-art performance, their accuracy downgrades severely on datasets with only a few labelled instances [56]. In various cases of rare diseases, it is difficult to acquire and annotate an adequate number of samples for large-scale training assignments. As a consequence, these models end up with poor generalization for novel classes given the low number of instances per class. Training a deep learning model in a low-data scenario results in a long-tailed and imbalanced classification, which is a challenging task in both computer vision and medical imaging [57]–[59].

Acquiring a large amount of labelled data for real-world problems including medical imaging and clinical diagnosis, is an exhaustive and expensive task. Therefore, it would be highly desirable to improve the learning strategies with the limited amount of available data. In this work, we explore the strategies to leverage the existing approaches for learning from limited data and build generalised models from relatively small samples. The main motivation to deal with the limited data in this research is the limited availability of datasets for rosacea.

IV. AVAILABILITY OF SKIN DISEASE DATASETS AND CHALLENGES

As deep learning models require a large amount of data for training, it is essential to benchmark the available datasets for skin disease analysis. In this study, we utilise datasets containing various skin disease images. These 17 datasets are also used in further sections where different types of deep Learning architectures and models are discussed in detail. The main purpose of this section is to provide an overview of the available skin image datasets, categorised by name, data source, disease category, imaging modality, dataset volume, number of classes, data accessibility, and the frequency of rosacea in existing datasets.

As shown in Table 3, there are only about 200 images of rosacea in publicly available datasets. Among the available images of rosacea, there is only a small number of images with the full-face visibility. Compared to the studies published based on skin cancer images, there is a very limited number of annotated rosacea images and that introduces a significant challenge in dataset split (train, validation and test) for training deep learning models. Hence, this study is focused on examining various deep learning techniques

TABLE 2. Overview of studies conducted on rosacea along with other skin conditions.

Author/ Index/ Year	Skin Disease Names	Dataset Name/ Source/ Availability	Dataset volume	Problem steps	Methodology	Performance measures	Deployment
Evgin Goceri [36], 2021	seborrheic dermatitis, rosacea, hemangioma, psoriasis and acne vulgaris.	DermWeb, DermNet Dermatoweb, DermQuest	Total no. of Images=725, No. of images for each class=145	Segmentation, Classification problem, Mobile App	Pre-trained on ImageNet weights: SqueezeNet, ShuffleNet, MobileNet, RMNv2, MobileNetv2, LightWeight Efficient Network (LWEN), Look-Behind Fully-CNN (LB-FCN), Light CustomNet2, ModifiedMobileNet2	Accuracy, Specificity, Sensitivity, Precision, F1 Score, Matthew's correlation coefficient (MCC)	32 GB RAM, Intel i9-9900 processor unit (3.10 GHz) and 64-bit Windows-10. Python 3.6, Java, Android Studio (version 3.6.1), TensorFlow
Thomsen *et al.* [31], 2020	acne (581) rosacea (1606), psoriasis (6,545), eczema (5,350) and cutaneous t-cell (2,461)	Department of Dermatology, Aarhus University Hospital (AUH), Denmark (Confidential Dataset)	Total images= 16,543 Total number of patients included in the study = 2,342	Classification problem, Region of interest using STN	Pre-trained on ImageNet weights with VGG-16 (VGG-16P), No pretrained VGG-16 (VGG-16N), Spatial Transformation Network (STN) with a Pre-trained VGG-16 Model (VGG-16PS), No pretrained VGG-16 with STN (VGG-16 NS)	AUC, sensitivity, specificity, negative predictive value (NPV), and positive predictive value (PPV), Accuracy	N/A
Evgin Goceri [39], 2021	seborrheic dermatitis, rosacea, hemangioma, psoriasis and acne vulgaris.	DermWeb, DermNet Dermatoweb, DermQuest.	N/A	Segmentation, Denoising, Intensity normalization, Fully Automated Detection of Facial Disorders (F-ADFD) method, Classification	Pretrained on ImageNet- VGGNet16, VGGNet19, GoogleNet, InceptionV3, Xception, ResNet18, ResNet50, ResNet101, InceptionResNetV2, DenseNet201with modified loss function (Cross-entropy and Tversky (Tv) similarity)	For segmentation- Area Error Rate (AER), For classification- Accuracy, Precision, Specificity, F1 score, MCC	Intel Core i7, 8GB DDR4 RAM, 3.6 GHz CPU, All networks have been trained using MATLAB (R2019b) on the same computer
Zhao *et al.* [32], 2021	3 rosacea subtypes (erythema-totelang-iectatic rosacea, papulo-pustular rosacea, and phymatous rosacea) acne, seborrheic dermatitis, and eczema	NA, Confidential Dataset, Data collection devices: iPhone X, Huawei P20 and digital camera Canon Rebel 550 from 3 different angles.	Total= 24,736, rosacea= 18,647; Acne, Seborrheic Dermatitis, eczema = 6089	Feature extraction, Classification	Pretrained on Imagenet-ResNet-50, mini-batch gradient descent witha momentum = 0.9, batch size = 32, Training epochs=100, Initial learning rate= 0.0001. (If validation loss did not decrease in continuous 10 epochs, the learning rate was divided by 5), minimum learning rate =0.000001.	Accuracy, precision, Area Under the Receiver Operating Characteristic Curve (AUROC)	N/A
Wu *et al.* [33], 2020	psoriasis (Pso), eczema (Ecz), atopic dermatitis (AD), healthy skin	Department of Dermatology, The Second Xiangya Hospital, Central South University, China, Confidential dataset	Total = 4,740 clinical images	Classification, Mobile App.	Five-fold cross-validation to validate the effectiveness, pre-trained weights on ImageNet, EfficientNet-b4 (380×380) The final fully connected classification layer was replaced with 3 output neurons. Also, added 7 auxiliary classifiers at the end of each intermediate layer to make the model learn classification information from different levels of features.	Positive rate (TPR), false positive rate (FPR), ROC, AUC, T-SNE analysis, Confusion matrix.	Pytorch 1.1. CPU - 18 Core Intel Xeon E5-2697, GPUs - 4 RTX 2080Ti NVIDIA.

TABLE 2. *(Continued.)* **Overview of studies conducted on rosacea along with other skin conditions.**

Author/ Index/ Year	Skin Disease Names	Dataset Name/ Source/ Availability	Dataset volume	Problem steps	Methodology	Performance measures	Deployment
Zhu *et al.* [34], 2021	14 diseases-lichen planus (LP), rosacea (Rosa), viral warts (VW), acne vulgaris (AV), keloid and hypertrophic scar (KAHS), eczema and dermatitis (EAD), dermatofibroma (DF), seborrheic dermatitis (SD), seborrheic keratosis (SK), melanocytic nevus (MN), hemangioma (Hem), psoriasis (Pso), port wine stain (PWS), basal cell carcinoma (BCC).	Department of Dermatology, Peking Union Medical College Hospital, China, Collected from October 2016 to April 2020, Confidential dataset The annotation process was performed by 2 dermatologists with more than 5-years' experience. Data collection device-MoleMax HD 1.0 dermoscope, Digital Image Systems, Vienna, Austria.	Total= 13,603 dermatologist-labeled dermoscopic Images, Rosacea=597 images	Classification and Clustering	Pre-trained weights on ImageNet, Google's EfficientNet-b4 (380×380) The final fully connected classification layer was replaced with 14 output neurons. Also, with added 7 auxiliary classifiers to each of the intermediate layer groups. t-SNE (t-distributed Stochastic Neighbor Embedding)	Area under curve (AUC), Accuracy, Sensitivity, Specificity, ROC, compared this model with 280 board-certificated dermatologists.	Pytorch Scikit-learn 0.22.2 and Numpy 1.16.4.
Pushkar Aggarwal [45], 2019	acne (332), atopic dermatitis (92), impetigo (138), psoriasis (280), rosacea (96).	DermNet NZ, Dermatology Atlas, Hellenic Dermatological Atlas and downloaded images from the Google search results.	Total = 938	Classification	Pretrained on ImageNet - Inception v3	Sensitivity, specificity, positive predictive value (PPV), negative predictive value (NPV), Matthew's correlation coefficient (MCC), and F1 score.	TensorFlow.
Binol *et al.* [46], 2019	rosacea lesions	Ohio State University (OSU) Division of Dermatology (Using DSLR camera), Confidential dataset	Total=41 facial images, The size of each image is 4608×3072	Image classification problem for rosacea and non rosacea lesions.	Pre-trained on ImageNet DCNNs: Inception-ResNet-v2, ResNet-101, Data Augmentation. Anatomically directed post-processing (APP) (Anthropometric model)	Dice coefficient, False positive rate.	MATLAB R2018b using the Deep Learning Toolbox, (HPC) with 128 GB RAM and 16 GB NVIDIA Tesla P100 PCI-E GPU
Xie *et al.* [47], 2019	80 skin diseases with each class have more than 100 images. (Includes rosacea).	Xiangya Hospital of Central South University Dataset is annotated by 20 professional dermatologists, Confidential Dataset, Data collection device: SONY DSC-HX50 (350dpi), CANON IXUS 50 (180dpi), NIKON D40 (300dpi), NIKON COOLPIX L340 (300dpi).	Total = 47,075 images were obtained using 4 types of digital cameras.	Classification.	Pretrained on ImageNet. Inception-ResNet-v2 (for 80 skin diseases classification) (Max training epochs=5000, basic learning rates=0.001, batch size=25, optimizer=Adam, and the loss function= categorical cross entropy). Inception V3, DenseNet121, Xception for comparative analysis.	Top-1 and Top-3 accuracies can reach 0.588 and 0.764. 4-fold cross validation.	3X NVIDIA TITAN Xp.

which may be applied for skin disease diagnosis and potentially suitable for dealing with a limited dataset.

V. A BRIEF OVERVIEW OF SKIN DISEASE ANALYSIS USING MACHINE LEARNING AND COMPUTER VISION METHODS

Considerable amounts of work on skin disease classification tasks have focused on computer-aided skin cancer diagnosis and classification support systems [78]–[82]. These non-invasive [80], [81], [83] methods, such as traditional image processing techniques, have been very popular and achieved notable results for skin disease diagnosis, particularly for skin cancer. The image processing techniques have been used to perform a broad range of image pre-processing, e.g. lesion segmentation and domain-specific feature extraction followed by classification tasks. Such diagnosis tasks use a small number of datasets [81]–[83]. Generally, these datasets contain less than a thousand sample images. Image classification problems that utilise small datasets, do not generalise well to new images i.e. a novel category of diseases or the classes with very small datasets.

Over the past few years, medical image classification has entered a new era thanks to the advancements of deep convolutional neural networks [30], [84], machine learning [85]–[87] and deep learning techniques [88]–[90]. These techniques do not require any hand-crafted features, but they heavily rely on high computational power [35], [91]–[93]. They are trained end-to-end directly from the image labels and raw pixels, with a single convolutional neural network for dermoscopic and clinical images [29].

Another principle that has attracted a lot of attention recently in the medical image analysis domain is transfer learning. The core idea behind Transfer Learning is to deal with fewer samples and is discussed in Section V.A.

Another approach is GANs. There have been a few studies on using GANs [94], [95] on medical image analysis [96] which are discussed in Section V.B. While exploring GANs has shown notable results, they come with a few limitations such as (1) mode collapse: when the generator collapses to map all latent space inputs to the same data and (2) instability: when different outputs are obtained for the same input. The principal causes for these phenomena are related to vanishing gradients through the optimization procedure [97]. However, when it comes to synthetic image generation of faces, a few types of GAN architectures have become successful as further discussed in Section V.B.

Given that GANs come with a few limitations and advantages, there is a scope to explore other subfields of machine learning to deal with limited datasets, such as meta-learning and few-shot learning [98]–[100]. Meta learning approaches differ from many standard machine learning algorithms. Meta learning systems are trained by being exposed to many tasks and are tested in their ability to learn new tasks. An example of a task might be classifying a new image within 7 possible classes, given one example of each class [99]. There has been a small number of studies based on meta learning and few-shot learning applied to medical images and skin disease diagnosis which are further discussed in Section V.C.

Advanced machine learning have been gaining popularity in the field of computer vision due to their advantages. Nevertheless, some of the traditional approaches in computer vision can be utilised when there is only a limited amount of data available. One of these approaches leverages the technique of 3D modeling. 3D face modelling is a computer graphics technique. By using an intuitive user interface several 3D face models can be created from one or more photographs [101]. Over the years various methodologies have been developed to reconstruct 3D faces, such as 3D Morphable Models [102], Active Shape Models [103]–[105], Gaussian Process Morphable Models [106], deep learning based reconstructions [107]–[109] and 3D modeling using GANs [110], [111]. However, there is only a small amount of literature available on medical image diagnosis and facial skin image diagnosis which will be discussed in Section V.D.

A. DATA AUGMENTATION AND TRANSFER LEARNING

Data augmentation is a technique to artificially create a new set of training data from the existing ones by a slight modification. This is a process of modifying and expanding the data through various geometric transformations and image processing tasks. For images like those of faces with rosacea, the geometry of the faces and the positions of affected regions on the faces are different in each image. These are known as positional biases. Data augmentation can work well with the positional biases present in images, in order to increase the size and quality of training datasets, especially with a facial dataset [112].

Humans learn from their experience, which helps them understand and solve new but similar tasks quickly. A similar kind of hypothesis is applied in a handful of algorithms and techniques [113]. Transfer learning is one of the deep learning approaches in which a new task, which is in a different but related category, can be learned and improved by acquiring experience from a previously learned task. Thus, the acquired learning experience comes from different constraints such as extracting features and fine tuning the model. These constraints play an important role along with monitoring the parameters of the model to obtain the desirable output.

This principle is used by Esteva *et al.* [29] to demonstrate a generalizable classification of a dermatologist-labelled dataset of 129,450 images including 3,374 dermoscopy images. A GoogleNet Inception version 3 CNN architecture [43] was pretrained on approximately 1.28 million images with 1,000 categories of real world objects from the 2014 ImageNet Large Scale Visual Recognition Challenge [92]. This model was fine-tuned on a skin cancer image dataset using transfer learning [113] to achieve 93.33% accuracy.

Table 4 presents an overview of the state-of-the-art studies which have utilised transfer learning and data augmentation principles for skin disease analysis.

The main points that can be drawn from the Table 4 are:

TABLE 3. List of accessible skin disease datasets.

Index	Dataset Name	Disease Categories/ Names	Imaging modality	Volume	Classes	Rosacea images	Accessibility	Country/ Region
1	7-point criteria (aka derm7pt) [60] 2019	Melanoma and non-Melanoma skin lesions	Clinical and Dermoscopic	>2000	∼20	0	Public	Canada, Italy
2	Asan and Hallym Dataset [61] 2018	12 types of Skin Cancerous lesions	Dermoscopic	17,125	12	0	Partially	South Korea
3	Dermatology ATLAS [62] 1999	All kinds of skin diseases (including rosacea)	Clinical	∼11,000	∼550	38	Public	Brazil
4	DanDerm [63] 1995	All kinds of skin diseases (including rosacea)	Clinical	>3,000	∼100	17	Public	Denmark
5	DermIS [64]	All kinds of skin diseases (including rosacea)	Clinical	∼7,000	∼700	49	Public	Germany
6	Dermnet Skin Disease Atlas [65]1998	All kinds of skin diseases (including rosacea)	Miscellaneous	∼23,000	N/A	0	Public	United States
7	Dermofit Image Library (aka Edinburgh Dataset) [66]	Cancerous skin lesions	Dermoscopic	1,300	10	0	Under License Agreement	Scotland,UK
8	DermNetNZ [13] 2016	All kinds of skin diseases (including rosacea)	Clinical and Dermoscopic	>25,000	>2,500	∼50	Public	New Zealand
9	Dermatoweb.net [67] 2002	All kinds of skin diseases (including rosacea)	Clinical and Dermoscopic	>7,300	0	45	Public	Spain
10	HAM10000 [68] 2018	Pigmented malignant and benign skin lesions	Dermoscopic	10,015	7	0	Public	Austria
11	Hellenic Dermatological Atlas [69] 2011	Common disease categories (including rosacea)	Miscellaneous	2,663	N/A	9	Public	Greece
12	ISIC [70] [71] 2016	Melanoma, seborrheic keratosis, benign nevi	Dermoscopic	>33,000	N/A	0	Public	Miscellaneous
13	MED-NODE [72] 2015	Melanoma and benign nevi	Microscopic	170	2	0	Public	Netherlands
14	MoleMap [73] [74] 2003-2015	Malignant and benign lesions	Clinical and Dermoscopic	>32,000	N/A	0	NA	New Zealand
15	PH2 Dataset [75] 2013	common nevi, atypical nevi, and melanomas	Dermoscopic	200 (80+80+40)	3	0	Public	Portugal
16	SD-128 [76] 2016	128 disease categories (Including rosacea)	Clinical	5,619	128 (>20 samples per class)	N/A	On request only	China
17	SD-198 [77]	198 disease categories (Including rosacea)	Clinical	6,584	198 (10-20 samples per class)	N/A	On request only	China

- Most of the work done using transfer learning for skin diseases analysis starts from 2016 onwards.
- Most of the studies were conducted on subtypes of skin cancer such as malignant melanoma and benign nevi. However, only a few studies related to rosacea were conducted so far. As seen in the Section II., most of the works on rosacea and facial skin conditions are conducted from 2019 onwards.

- Most studies used a minimum data volume of 1000 images. A small number of studies have been conducted with less than 1000 images.
- The studies by Esteva *et al.* [29], Liu *et al.* [114] obtained an accuracy of 93.33% and 93% respectively with a large number of images and used InceptionNet-v3 [43] and v4 [41] respectively. The studies by Goceri [115], MAA [116], Cui *et al.* [117] used a small number of images to train an Inception Net [43] model. There are a few studies with a small number of datasets that obtained results by using different versions of the VGG16 [38] and ResNet [44] architectures with transfer learning, data augmentation and some pre-processing work.

Similarly, Yu *et al.* [118], Kwasigroch *et al.* [119], Lopez *et al.* [120], Kassani *et al.* [121] presented studies on cancerous dermoscopic skin lesions classifications using DCNNs with transfer learning. Some of these works are done using InceptionNet-v3 [43] and VGG-Net [38].

Shorten *et al.* [112] discussed a few limitations on data augmentations such as:

- Finding the optimum final post-augmented dataset size to produce the best performing model. There is a possibility that the augmented dataset can be heavily biased.
- There are no existing augmentation techniques that can correct a training dataset with very poor diversity with respect to the testing data. All the augmentation algorithms perform best under the assumption that the training data and testing data are both drawn from the same distribution. Hence, these limitations in data augmentation could be a potential problem for small medical image datasets because of class imbalance and diversity.

Morid *et al.* [122] systematically reviewed the literature on approaches to transfer learning in medical image analysis that are based on CNN models trained on the non-medical ImageNet dataset for medical image analysis. A vital research gap discussed in this review is finding the optimal dataset size that can support medical image analysis tasks, as a large dataset may not always be available.

An extensive survey published by Pan *et al.* [113] discusses a few limitations on transfer learning that may apply to medical image analysis, such as negative transfer, which is an open problem in transfer learning. For example, when using the ImageNet [35] dataset for medical/clinical image analysis, there is no similarity between the source and target domains. ImageNet contains real-world objects, animals, fruits, balloons etc. Hence there is a high possibility of performance intrusion in the target domain; which is known as negative transfer [123]. Negative transfer is made more likely by the fact that well performing CNN models are pre-trained on a non-medical dataset [122]. In simple words, it is not yet established that,

- Which characteristics facilitate an effective transfer of features and weights in the transfer learning and fine-tuning process?
- Whether the features that are transferred from ImageNet are plausible or not?
- If the transferred features and weights are plausible, then how can we quantify that?
- At what level is it adequate to incorporate the features of a non-medical dataset during the training process?

Considering the limitations of transfer learning and data augmentation, this study has considered a few methods such as GANs, 3D modelling and meta-learning with few-shot classification to improve medical image diagnosis of rosacea and other facial skin conditions using AI and computer vision.

B. GENERATING SYNTHETIC IMAGES USING GANs

As discussed in the previous Section V.A., data augmentation techniques are used in various studies, but there are a few notable limitations. Although data augmentation techniques help in transforming the images by zooming, cropping, flipping, rotating, it does not radically improve results when there is only a handful of data available for some specific skin conditions. However, GANs can be explored in creating synthetic data from an existing limited dataset without splitting the dataset into training, validation, and test sets.

Generative models are inspired by the unsupervised learning model approach. They can generate new examples that are similar to the training images. The GAN framework [95] consists of a pair of adversarial networks – a Generator Network G and Discriminator Network D. The Generator Network G tries to transform random noise from the prior distribution over the input variables (usually a standard normal distribution/gaussian distribution) to generate fake/synthetic images which look as realistic as possible. The input variables to G are drawn from a normal distribution and the output is a synthetic image. Generally, the dimension of the output image is much greater than the dimension of the input variables.

Simultaneously, a Discriminator Network D attempts to discriminate between the sample images obtained from the real training data and the fake/synthetic images obtained from the generator function G. By utilizing the feedback from the discriminator D, the parameters of the generator G can be adjusted such that its samples are more likely to fool the discriminator network in its classification task. Ultimately, it is desired that the distribution of the fake images has as much in common as possible with the real images. In the Discriminator Network D, the input is an image, and the output is a real number between 0 and 1, which represents the probability that the input image is real. Ideally if D is working properly, the output will be close to 1 for a real image and close to 0 for a synthetic one.

The equation below represents the function V which GANs optimise during training. x_{real} represents a real image. z represents the random input values for G. In this equation, the first term only applies to real data and the second term only applies to the synthetic data.

$\mathbb{E}_{x\sim p_{data}(x)}$ indicates the expected value of $\log(D(x_{real}))$ where $p_{data}(x)$ is the probability distribution over the real data and $\mathbb{E}_{z\sim p_z(z)}$ is the expected value of $\log(1 - D(G(z)))$ where $p_z(z)$ is the probability distribution over the input values to G. The parameters of G and D are optimized by playing a

TABLE 4. Studies based on data augmentation and transfer learning.

Author/ Index/ Year	Skin Disease Names	Dataset Name/ Source	Dataset volume in total/per class	Methodology	Best results and Performance measures
Esteva *et al.* [29], 2017	2,032 skin diseases for Training the model and Tested for malignant melanomas, benign nevi, malignant basal, squamous cell carcinomas, intraepithelial carcinomas, pre-malignant actinic keratosis, benign seborrheic keratosis.	ISIC Dermoscopic Archive, Edinburgh Dermofit Library and data from the Stanford Hospital.	1,29,450 images. 2,032 disease classes for Training and 7 types of cancerous lesion classes for Testing.	Pre-trained on ImageNet dataset Transfer Learning, Data Augmentation, InceptionNet-v3.	Accuracy =93.33%, Confusion matrix Saliency Maps, Sensitivity-specificity curves.
Sourav Mishra *et al.* [124], 2018	9 common skin conditions: Acne, Alopecia, Crust, Erythema, Leukoderma, Pigmented Maculae, Pustule Ulcers and Wheal.	N/A	Each class comprises of approximately 4600 images in which the division between training and test ratio of 90:10	Pre-trained on ImageNet DCNNs such as: ResNet18, ResNet50, ResNet152, DenseNet161.	Classification accuracy: 82.30%(by ResNet152)NVIDIA Titan XP and CUDA v8
Binol *et al.* (RosNet) [46], 2019	Rosacea lesions	Ohio State University (OSU) Division of Dermatology (using DSLR camera)	41 facial images. The size of each image is 4608×3072	Pre-trained on ImageNet DCNNs: Inception-ResNet-v2, ResNet-101, Image classification problem for rosacea and non-rosacea lesions, Data Augmentation, Anatomically directed post-processing (anthropometric model)	Dice co-efficient: 92.9% False positive rate, MATLAB R2018b using the Deep Learning Toolbox, (HPC) with 128 GB RAM and 16 GB NVIDIA Tesla P100 PCI-E GPU.
Goceri. [115], 2019	5 common skin diseases; (1) Acne vulgaris, (2) Hemangioma, (3) Psoriasis, (4) rosacea, and (5) Seborrheic dermatitis.	N/A	Total = 800, Per class= 160	Pre-trained on ImageNet: U-net, InceptionNetV3, InceptionResNetV2, VGGNet and ResNet.	Classification Accuracy: 80% (by ResNet50). GeForce GTX 980Ti GPU, Intel Core i7-4930 K processor, 6GB memory and 16GB RAM
Sun *et al.* [76], 2016	198 Common skin diseases: eczema,psoriasis, acnevulgaris, pruritus, alopecia areata, decubitus ulcer, urticaria, scabies,impetigo, abscess,bacterial skin diseases, viral warts, molluscum, melanoma and non-melanoma skin cancer	SD-198 and SD-128	total= 6,584; for some classes-10 to 20 samples.	Pre-trained on ImageNet DCNNs such as: CaffeNet, CaffeNet+ fine-tuning, VGG Net, VGG Net + finetuning	Classification accuracy: 50.27% (by VGGNet + fine-tuning)
Yang *et al.* [125], 2018	198 common skin diseases.	SD-198	6,584; for some classes-10 to 20 samples.	Pre-trained on ImageNet DCNNs such as: GoogleNet, GoogleNet + fine tuning, ResNet, ResNet + fine tuning	Classification accuracy: 53.35 % (by ResNet +fine tuning)
MAA [116], 2019	Seven skin diseases-Melanoma (1113), Melanocytic nevus (6705), Basal cell carcinoma (514), Actinic keratosis (327), Benign keratosis (1099), Dermatofibroma (115) and Vascular (142).	ISIC 2018 Melanoma Detection Challenege and Dataset	Training set = 10015 skin lesion images. The validation dataset = 193 skin lesion images.	Data Augmentation. Representation learning. Pre-trained on ImageNet DCNNs with fine tuning such as: PNASNet-5-Large, InceptionResNetV2, SENet154, InceptionV4, An Ensemble of all models.	Validation score: 76% (by PNASNet-5-Large)
W.Sae-Lim *et al.* [126], 2019	Seven skin diseases: Cancerous	Human Against Machine 10,000 (HAM10,000)	10,015 images	Pre-trained on ImageNet Modified Mobile-Net with Data Augmentation Data up-sampling.	Accuracy: 83.23%, Specificity: 87%, Sensitivity: 85%, F1 score:82%
Kemal *et al.* [127], 2020	Seven skin diseases: Cancerous	HAM10,000	10,015 images	A CNN architecture + One verses all which 1,243,463 parameters in total. Data Augmentation.	Average precision: 92.90%
Hosny KM *et al.* [128], 2019	Melanoma skin lesions.	(i)2017 ISIC challenge dataset, (ii)MED-NODE, (iii)DermIS+ DermQuest.	2000, 170, 206	Data Augmentation Pre-trained on ImageNet for transfer learning on AlexNet	Average Accuracy: 95.91%, 96.68%, 97.07%.
Mahbod *et al.* [129], 2019	411 malignant melanoma (MM), 254 seborrheic keratosis (SK) and 1372 benign nevi (BN)	ISIC 2016, ISIC 2017	Total= 2037, Training= 1887, Validation set=150	multi-class non-linear support vector machine (SVM) classifiers. Fusion of DCNNs such as AlexNet+ VGG16+ ResNet18)	Average AUC:90.69%

TABLE 4. ***(Continued.)*** **Studies based on data augmentation and transfer learning.**

Author/ Index/ Year	Skin Disease Names	Dataset Name/ Source	Dataset volume in total/per class	Methodology	Best results and Performance measures
Mendes *et al.* [130], 2018	11 distinct lesions with 4 malignant illness.	(i)MED-NODE, (ii)Edinburgh Dermofit library, (iii) Atlas	(i)170, (ii)1,300, (iii)3816	Data Augmentation, Pre-trained on ImageNet DCNNs: ResNet-152	Total accuracy: 78% (by ResNet-152)
Cui *et al.* [117], 2019	Melanoma (295) and non-melanomas (311)	International Society for Digital Imaging of the Skin (ISIC).	Total= 606	Image pre-processing segmentations, feature extractions, Machine Learning classifications-using SVM, Regression tree, K-nearest neighbour, Logistic regression, Transfer Learning using-AlexNet, VGG16, VGG19, Google Inception v3.	Average accuracy, Sensitivity, Specificity. (Accuracy, Sensitivity, Specificity=93.70%, 95.30%, 92.10% respectively by Inception v3), Windows 7 system, MATLAB R2018b, TensorFlow 1.3, GTX1080Ti (Nvidia).
Liu *et al.* [114], 2020	26 most common skin conditions in adult, by making it 419 categories of skin conditions (Rosacea is not included), Labeled by a cohort of 37 US board-certified and 5 Indian board-certified dermatologists.	Tele Dermatology consultation dataset (Confidential)	Training=64,837, Validation=11,268, clinical metadata (demographic information and medical history)	Transfer Learning pretrained on ImageNet, Fine tuning, Inception v4, Data Augmentation	top-3 accuracy=93% -top-k sensitivity=83% -95% confidence intervals, -validated by 18 board certified dermatologists who did not participate in labelling the input images.

minimax game, which involves varying the parameters of G to minimise V in an outer loop and varying the parameters of D to maximise V in an inner loop. The value function $V(G, D)$ is defined as:

$$\min_G \max_D V(D, G) = \mathbb{E}_{x\sim p_{data}(x)}[\log(D(x))] + \mathbb{E}_{z\sim p_z(z)}[\log(1 - D(G(z)))] \quad (1)$$

At the early stages of the learning process, G will not be generating any realistic looking images and D can reject samples with high confidence because they are clearly different from the training data. In this case, $\log(1-D(G(z)))$ should be close to zero because $D(G(z))$ will be close to zero [94], [95].

In skin disease classification and analysis, there have been a few impactful studies, which support generating synthetic images from existing datasets of real images to increase the training samples and improve the classification accuracy. These studies will be considered as a part of a critical analysis and are listed in Table 5.

The main points that can be drawn from Table 5 are:

- Most of the work on GANs for skin diseases classification is from 2018 onwards.
- Most of the diseases considered for generating the synthetic image dataset are melanoma or cancerous skin lesions. There is no work related to rosacea or any facial skin conditions.
- Minimum of 2,000 input real images are considered for generating synthetic images.
- Majority of the works use the ISIC 2017 and 2018 datasets.
- DCGAN, PGAN and LAPGAN appear to be popular architectures used in these studies.

Qin *et al.* [131] states that the generation of synthetic samples for vascular lesions (142 input images) makes the lesion region look realistic. However, the skin texture around the lesion is still fuzzy and lacks contrast in some samples. The same effect appears in melanoma images. For melanocytic nevus (6705 images), the most representative images are with concentrated colour, clear edge and regular shape. Hence, more training samples lead to generating better quality synthetic ones. In Rashid *et al.* [132], the highest F1 score was obtained in the melanocytic nevus (6705 images) category because of the high number of samples available.

1) MAJOR TAKEAWAYS ON DCGAN, LAPGAN AND PGAN

DCGAN [133] and LAPGAN [134]have proven to work well for generating synthetic images from the input noise, but the generated images were low in resolution e.g. 64 × 64 px. This setting can be improved using conditional GAN approaches [135]. Recently, the Progressive Growing of GANs (PGAN) [136] has shown promising results for realistic image synthesis of faces at resolutions up to 1024 × 1024 px, without the need for any conditioning. In simple words, conditioning is the way of feeding additional information to the generator and discriminator. It can be useful when dealing with an imbalanced dataset. Baur *et al.* [137], [138] shown that the synthetic sample images produced by DCGAN are prone to checkerboard artefacts and they can be easily identified as fake. The sample images produced using LAPGAN are realistic and diverse, but the close inspection of the images shows a vast amount of high-frequency artefacts. The generated samples using PGAN seem highly realistic, and it is trained without considering the presence of various classes. However, the presence of hair in the skin images may raise questions. Hence PGAN and LAPGAN can be taken into consideration in our further studies to generate synthetic images of faces with rosacea. However, there are a few

research gaps which are discussed by Baur *et al.* [137], [138] including:

- Whether there is an information gain in the synthetic samples over the actual training dataset?
- Whether the gain is higher than using conventional data augmentation?
- How many training images are required to obtain reliable generative models?
- There is still a need to enhance the methodology to account for filamentary structures.

2) STYLE-BASED GENERATIVE ADVERSARIAL NETWORKS

To examine a specific facial skin condition such as rosacea, it is necessary to access full face images with anatomical details. Therefore, a GAN model should be trained to generate full facial synthetic images rather than partial facial images. The Style-based GAN [146] is an improvement of PGAN, which supports generating higher-quality images via the incremental expansion of both generator and discriminator models for low quality to high quality images. Looking at the state of the art, Bissoto *et al.* [145] shown promising results with StyleGAN2 [147]. This work also suggests noise-based GANs work better than translation based GANs such as Pix2pixHD [148] and SPADE [149].

Chai *et al.* [150] looked at one of the open questions on GANs which aims to look at how to convert unstructured latent code to a high quality output while maintaining global consistency. They show that StyleGAN [146] performs better in separating faces from background artifacts. Subsequently, StyleGAN2 [147] was introduced as an improved version of StyleGAN, hence StyleGAN2 can be considered for obtaining relatively high-quality synthetic facial images with global consistency of anatomical details and affected regions of the face. StyleGAN2 works better in comparison to PGAN. However, StyleGAN2 takes up to one month of GPU time for a single course of training. Additionally, StyleGAN2 also produces high quality facial images [147], which can be useful for generating synthetic face images with facial diseases. Recently, StyleGAN2 with adaptive discriminator augmentation (StyleGAN2-ada) [151] has been introduced, which claims to help with relatively limited data (a few thousand training images) regime due to an adaptive discriminator augmentation mechanism which does not require changes to the network architecture or defined loss functions. This may help in generating images with a few hundred samples. As StyleGAN2-ada has acquired optimal results with Flicker Faces-HQ dataset [146], which is basically a facial dataset, it may help in generating synthetic images of facial skin conditions e.g. rosacea.

C. META-LEARNING AND FEW-SHOT CLASSIFICATION

The concept of meta-learning and few-shot classification can help deal with the limited amount of data without any transfer learning techniques, and without any augmentation process (such as synthetic image generation) of the dataset, but through hyperparameter optimization.

In a meta-learning problem, we have a meta-training set and a meta-test set, each of which contains a number of "tasks". Each task is associated with a training set and a test set containing both feature vectors and correct labels. It is similar to a standard machine learning problem but each task is considered as one data sample [98]. The goal of meta-learning is to acquire generic knowledge of different tasks. The knowledge can then be transferred to the base level learning to provide generalisation in the context of a single task [152].

Meta-learning assumes that all the tasks in both the meta-training set and the meta-test set, have some degree of similarity. For example, in the case of skin diseases the meta-training tasks might represent different, well-studied skin conditions and the meta-test set might represent a rarer skin condition, for which there is limited data.

Regular machine learning involves the minimisation of a loss function $\mathcal{L}$.

$$\theta_C^* = \arg\min_{\theta} \mathcal{L}(\theta_C, D^{tr}) \tag{2}$$

where θ_C is a vector of the parameters of a classifier (e.g. the weights of a neural network). The classifier takes an input x which represents the feature values of an example and outputs a label y.

Meta-learning involves estimating the parameters θ of a "learning function" f_θ. The learning function takes as input a training set D_i^{tr} and outputs a vector ϕ_i as in Equation. 3 below.

$$\phi_i = f_\theta(D_i^{tr}) \tag{3}$$

ϕ_i can be used to generate a classifier, which can classify examples from the corresponding test set D_i^{ts} for task i.

Meta-learning involves minimising the function in Equation. 4 with respect to θ,

$$\theta^* = \arg\min_{\theta} \sum_{i=1}^{n} \mathcal{L}(\phi_i, D_i^{ts}) \tag{4}$$

where n is the number of tasks in the meta-training set. For each task i a vector ϕ_i is generated using the learning function f_θ as in Equation. 3 above. The same learning function (with the same values for θ) is used for all tasks.

Then ϕ_i is used to generate a classifier, which can then applied to the test set D_i^{ts} to generate labels for each example in the test set. The loss function $\mathcal{L}$ is calculated by comparing the generated labels with the true labels. The loss functions for all the tasks in the meta-training set are then summed. An optimisation algorithm is then used to find the values of θ which minimises the function in Equation. 4.

Fig. 2 is an example of a meta-learning setup. The figure represents the meta-training set and the meta-test set, where each grey rectangle is a separate task that consists of a training set and a test set separated by the dotted lines. The training sets are also called support sets. The test sets are also called query sets. Each image is taken as one example within the dataset. Each training/support set has 5 different example

TABLE 5. Studies based on GANs.

Author/ Index/ Year	Skin Disease Names	Dataset Name/ Source/	Dataset volume in total/per class	Methodology/Benchmark	Best results Evaluation Metrics /Samples Generated, Deployment and H/W
Qin *et al.* [131], 2020	Seven skin diseases-Melanoma (1113), Melanocytic nevus (6705), Basal cell carcinoma (514), Actinic keratosis (327), Benign keratosis (1099), Dermatofibroma (115) and Vascular (142)	International Skin Imaging Collaboration (ISIC) 2018	10,015 dermoscopic images. 600×400 pixels and 96dpi.	Transfer learning and fine tuning on Transfer-ResNet50, GAN, DCGAN, StyleGAN, SL-StyleGAN(proposed work), Non-linear mapping network, Adaptive Instance Normalization (AdaIN)operations, Style Mixing, Stochastic variation	Inception Score, Fréchet Inception Distance (FID), Precision and Recall. Best result obtained by SL-StyleGAN proposed method. H/W: Intel Xeon Gold 6144 with 192 GB RAM, GPU of NVIDIA Quadro P40 0 0.
Lei *et al.* [139], 2020	Melanoma skin lesions	International Skin Imaging Collaboration (ISIC) Skin Lesion Challenge Datasets 2016, 2017 and 2018	ISIC2016: Training-900, Test-379; ISIC2017: Training-2000, Testing-600; ISIC2018: Training-2296, Testing-300	Segmentation task, A deep encoder-decoder module UNet-SCDC (skip connection and dilated convolution) (proposed work), Dual discrimination module.	Accuracy, Sensitivity, Specificity, Jaccard Index, Dice coefficient, H/W: Two NVIDIA TITAN XP GPUs.
Baur *et al.* [137], 2018.	Benign and malignant skin cancerous lesions	ISIC2017	2000 (256×256px)	DCGAN, LAPGAN, deeply discriminated GAN (DDGAN) (proposed work), Tranfer learning: pretrained ResNet-50	Earth mover's distance (MD) (Wasserstein-Distance), JS Divergence, 2000 random samples generated. H/W: NVidia 1080Ti
Rashid *et al.* [132], 2019	Melanoma (MEL); Melanocytic Nevus (NV); Basal Cell Carcinoma (BCC); Actinic Keratosis (AKIEC); Benign Keratosis (BKL); Dermatofibroma (DF); Vascular Lesion (VASC)	ISIC2018	8,000 training images, 2,000 testing images.	Transfer learning, Finetuning, DenseNet, ResNet50, GAN based augmentation	Precision and Recall, F1 score, Balance accuracy score: 0.86 using GAN based augmentation, Highest F1 score for Melanocytic Nevus (NV).
Baur *et al.* [138], 2018	Benign and malignant skin lesions of 7 categories.	ISIC2018	10,000 labelled training samples	PGAN, DCGAN, LAPGAN, Visual Turing Test	Sliced Wasserstein Distance (SWD): 20.0197 (closest to the lower bound, 10,000 synthetic images generation per model, User study amoung 3 expert dermatologists and 5 Deep Learning experts; showing experts had a hard time distinguishing real and fake image
Bisla *et al.* [140], 2019	Three classes: melanoma, nevus, and seborrheic keratosis.	ISIC 2017 (3 classes) PH2 (2 classes), Edinburgh Dataset, Test dataset: ISIC 2017 and ISIC 2018	803+40+76 cases of melanoma, 2107+ 80+ 331 cases of nevus, and 288+ 257 cases of seborrheic Keratosis from ISIC2017, PH2 and Edinburgh Dataset respectively	Segmentation using U-Net architecture, de-coupled DCGANs for data generation, Pre-trained ResNet-50 for final classification.	MSE for GANs, 350 synthetic images for melanoma and 750 synthetic images for seborrheic keratosis (26% artificially generated data for training) ROC and AUC for classification.
Bissoto *et al.* [141], 2019	Melanoma skin lesions	ISIC 2017 Challenge, ISIC Archive, Dermofit Image Library, PH2 Dataset, For Test: Interactive Atlas of Dermoscopy	2,000, 13,000, 1,300, 200, 900 dermoscopic images of 270 melanomas categories.	SLIC algorithm, DCGAN, Conditional PGAN, pix2pixHD GAN (a conditional image-to-image translation GAN) using only semantic map, Real+Instance+PGAN	AUC, p-value

TABLE 5. ***(Continued.)*** **Studies based on GANs.**

Author/ Index/ Year	Skin Disease Names	Dataset Name/ Source/	Dataset volume in total/per class	Methodology/Benchmark	Best results Evaluation Metrics /Samples Generated, Deployment and H/W
Pollastri *et al.* [142], 2019	Melanoma Skin lesions	ISIC 2017	1882 (As Authors wished to remove 118 images from the dataset	Segmentation task using Baseline CNN architecture and U-Net, DC-GAN, LAPGAN	Jaccard Index
Ghorbani *et al.* [143], 2020	26 skin conditions (no rosacea) Melanocytic nevus, Melanoma and Seborrheic Keratosis/Irritated Seborrheic Keratosis, Scar condition, Basel cell Carcinoma etc.	Tele-dermatology service dataset: collected in 17 clinical sites in two U.S. states from 2010 to 2018	9,897 cases and 49,920 images; each case contains one or more high resolution images (resolution range: 600×800 to 960×1280).	Pix2pix GAN architecture, Human Turing Test, DermGAN, MobileNet	20,000 synthetic images are generated using the 8-class DermGAN model and added them to the existing training Data to train MobileNet.
Romsaas *et al.* [144], 2020	Benign and Malignant cancer lesions	ISIC 2019	Total= 25,331 images. With 7 classes.	ACGAN (128×128), CycleGAN (256×256), Path-Rank-Filter (to generate class specific synthetic images)	Upto 24,000 synthetic images are generated using ACGAN and CycleGAN, Precision/recall, Maximum Accuracy = 86%
Bissoto *et al.* [145], 2021	Benign and malignant cancer lesions	ISIC 2019, ISIC 2020, Derm-7pt-dermoscopic, Derm-7pt-clinical, Dermofit.	3,863, 1,743, 872, 839, 973	PGAN and StyleGAN2 (to generate from random noise), pix2pixHD and SPADE (for semantic segmentation masks to guide the generation), Inception-v4 for classification, Data Augmentation.	Fréchet inception distance (FID) "StyleGAN2 performed ahead of all other GANs".

images, and each test/query set has 2 additional example images. The meta-learning model can be trained on the tasks in meta-training set and then tested on entirely new tasks in the meta-test set. The whole dataset is divided and structured as shots/iteration/episodes.

Few-shot classification is a subset of meta-learning. ''Few-shot learning'' means learning a large number of tasks using datasets containing only a few examples known as 'shots', e.g. training five different classes where each class has just one example is called 1-shot-5-way classification. Fig. 2 is an example of a 1-shot-5-way classification task (the word 'way' indicates a class). The main idea of few-shot meta-learning is to train a few iterations/shots from the whole dataset, so the model can quickly adapt to the new task with only fewer examples. In order to attain this idea, the meta-learner is trained over a large set of different tasks, such that for the new unseen tasks, the model can learn quickly with only a limited number of examples. In effect, the meta-learning problem treats an entire dataset as training examples [99], [100]. The whole dataset is divided and structured as shots/iteration/episodes.

There are three general meta-learning categories including: Model-based (Black-Box) Meta-Learning, Metric-based (Non-parametric) Meta Learning, Gradient-based (Optimization-based) Meta Learning. Typical architectures that are model-based meta learning are Memory Augmented Neural Network (MTNN) [153], Meta-Net [152], Simple Neural AttentIve Learner (SNAIL) [154]. Typical architectures that are metric-based meta learning are: MatchingNets [155], RelationNet [156], FSL with Graph Neural Networks [157], Prototypical Networks [158]. Typical architectures that are gradient-based meta learning are: MAML [100], Reptile [159], Auto-Meta [160], GIMLI [161], ALFA [162]. The Model-based meta-learning is conceptually very simple, but it has minimal inductive bias, meaning everything must be meta-learned. However, metric-based meta-learning can work very effectively by combining some inductive bias with easy end-to-end optimization and is restricted to classification models. On the other hand, optimization-based meta-learning is convenient to apply any architecture and good at generalizing a wide range of domains. An overview of the state-of-the-art studies on skin disease analysis using meta-learning and few-shot learning is presented in Table 6.

A few other studies on meta learning and few-shot learning for other domains of medical image analysis shown promising results. Zhao *et al.* [163] proposed a novel approach for automating data augmentation for synthesizing labelled MRI brain scans. The proposed method only requires a single segmented scan. This approach uses a semi-supervised method for dealing with unlabelled scans that results in a major improvement over bio-medical image segmentation state-of-the-art methods.

Guo *et al.* [164] and Zhao *et al.* [56] showed a comparative study among different CNN architectures using meta-learning and few-shot learning algorithms in various medical image analyses. Patacchiola *et al.* [165] proposed Deep

FIGURE 2. An example of Meta-Learning set up in 1-shot-5-way classification.

Kernel Transfer (DKT) which is a Bayesian treatment for the inner loop through deep kernels in the meta-learning algorithm. This approach has many advantages such as, (a) it is simple to implement as a single optimizer, (b) it offers uncertainty quantification, and (c) it does not need estimation of task-specific parameters.

Cai *et al.* [166] proposed a novel score-based meta transfer-learning to address the cross-domain few-shot learning problem. This work claims to achieve an average accuracy of 74.06%, which significantly outperforms previous best-performing meta-learning and transfer-learning methods by 14.28% and 5.93%. Sun *et al.* [167] have proposed a novel few-shot learning method called Meta-Transfer Learning (MTL) which learns to adapt a DNN for few-shot learning tasks.

The datasets used in this work are miniImageNet (100 classes with 600 samples per class) and Fewshot-CIFAR100 (100 classes with 600 samples per class). Compared to other few-shot learning methods, MTL has shown remarkable results in low data settings. In a few-shot learning pipeline, Gidaris *et al.* [168] used self-supervision as an auxiliary task, that allows feature extractors to learn richer and more transferable visual representations while using few annotated samples. Hospedales *et al.* [169] reviewed many existing works in various domains. They claim that there is still a gap in understanding which kinds of meta-representations tend to generalize better under certain types of domain shifts. Wang *et al.* [170] looked at various studies on a few-shot learning approach in which it is said that real-world computer vision tasks with low data situations are the first test-bed for few-shot learning algorithms. It is also seen in various works that transfer learning methods are used in a few-shot learning approach as part of the domain adaption, which might be beneficial in case of limited data availability across the medical image analysis domain.

D. 3D FACE MODELLING

There have been a few preliminary studies on 3D modelling of faces and other biomedical images using Statistical Shape Models (SSMs) which include Active Shape Models (ASMs) [103], [105] and Active Appearance Models (AAMs) [104]. Mainly, MRIs of the brain and knees have been considered in depth in these works while other medical applications were also mentioned. The ASM essentially matches a model to boundaries in an image. The AAM finds model parameters that synthesize a complete image similar to the target image by using a set of target feature points. The combination of shape and appearance has turned out to be very impactful [102]. The better the model represents the structure of the objects to be analyzed, the easier it becomes to fit the model. Due to the linear and parametric nature of SSMs, they are mathematically convenient and easy to

TABLE 6. Studies based on meta learning and few shot classification.

Author/ Index/ Year	Skin Disease Names	Dataset Name/ Source/	Dataset volume in total/per class	Methodology/Benchmark	Best results/ Evaluation Metrics /Samples Generated, Deployment and H/W
Li *et al.* [171],2020	Melanocytic nevus (6705), melanoma (1113), benign keratosis (1099), basal cell carcinoma (514), actinic keratosis (327), vascular lesion (142) and dermatofibroma (115). squamous cell carcinoma, haemangioma, and pyogenic granuloma	ISIC2018 Skin Lesion Dataset, Dermofit Image Library (for validation)	10,015 First four diseases for training and the remaining 3 are for testing	Difficulty aware meta learning (DAML) framework, Transfer learning.	AUC: 83.3% (for 5 samples per class).
K. Mahajan *et al.* [172], 2020	Dermoscopy images eczema, acne, and various cancerous conditions.	ISIC 2018, Derm7pt, SD-198	10,015 (7 classes), 2,000 (20 classes), 198	Reptile (Gradient based meta learning),Prototypical networks (Distance metric based meta learning technique which computes a prototype vector as the representation of each class), G-convolutions (group equivalent convolutions), 2-way classification.	For ISIC2018: AUC: 86.8 (using Reptile, G-conv, 5-shot) For Derm7pt:AUC: 77.2 (using Reptile, G-conv, 5-shot)For SD-198:AUC: 89.5 (using Reptile, 2-way G-conv, 5-shot)
Zhang *et al.* [173], 2020	Melanocytic nevus (6705), melanoma (1113), benign keratosis (1099), basal cell carcinoma (514), actinic keratosis (327), vascular lesion (142) and dermatofibroma (115)	ISIC2018	10,015(7 classes) 4 classes with the largest number of samples for training and the remaining 3 classes with relatively fewer number of samples for testing.	Fine tuning and data augmentation, MAML (Model Agnostic Meta Learning), ST-Meta Diagnosis Network, A few shot settings (3ways1shot, 3ways3shot and 3ways5shot) with different STN (Spatial Transform Network) modules stacked up into different layers.	Average Accuracy: 81.38%.
Fayjie *et al.* [55], 2020	Miscellaneous	FSS-1000 (Base Training set), ISIC 2018, PH2 dataset	1000 classes where each class contains 10 images, 2594 dermoscopic images with their respective masks 200 RGB dermoscopic images of melanocytic lesions.	Segmentation task, Pretrained VGG network on ImageNet is used as Encoder, A few shot learning with 'support' and 'query' set, The pretrained VGG network architecture from ImageNet is used as an encoder, Atrous convolutions with dilation rate 2 are incorporated with episodic training.	DSC (Sørensen–Dice coefficient)score, The proposed approach outperforms the few-shot baseline by a margin between 6-7%, H/W: Keras with Tensorflow using the Nvidia Titan X GPU.
Zhao *et al.* [56], 2020	Miscellaneous (no rosacea)	miniImagenet (source domain) Crop Diseases dataset, EuroSAT, ChestX and ISIC 2018 (target domain datasets)	N/A	Few-shot learning, Baseline fine tuning method, BSR (Batch Spectral Regularization) with data blending, BSR with LP (Label Propagation), BSR with data blending in Ensemble, BSR with data blending and with LP in the Ensemble network	Best-Average Performance results are obtained by BSR with data blending and with LP in Ensemble network architecture using 5-way 50-shot.

work with image analysis algorithms. For this reason, SSMs have become very popular [106]. However, SSMs come with various drawbacks such as (a) the shape variation in SSMs is restricted to the linear span of the training data, (b) hence, a lot of training data is needed.

The application of computer vision for face modeling has focused on the direction of a new face representation using analysis-by-synthesis [174]. This seeks to explain an image by synthesizing its content using both 2D and 3D modelling. One technique which does this is 3D Morphable Models (3DMMs) [101].

A 3D Morphable face model is based on the two fundamental ideas (a) all faces are in dense point-to-point correspondence (which is usually established on a set of example faces in a registration procedure), (b) this correspondence can be maintained throughout any further processing steps [102]. A 3DMM is a generative model which applies to the entire shape of the face and the appearance of the face.

2D morphable models and 3D morphable models rely on dense correspondence rather than only a set of facial feature points [102]. Determining the dense correspondence is only possible by assigning every point on the reference object that

FIGURE 3. Standard reference shape. This image is taken from the work by Lüthi *et al.* [106].

(a) $s = 100$, $\sigma = 100$ mm

(b) $s = 10$, $\sigma = 30$ mm

FIGURE 4. Generated face models using a Gaussian Covariance function with different standard deviations. This image is taken from the work by Lüthi *et al.* [106].

is semantically meaningful to the corresponding point on the target object. This process is called image registration. The same anatomy of an object can be explained using any other object of the same class perturbed with deformation or slight structural variation [175]. The generalization of SSMs is called Gaussian Process Morphable Models (GPMMs) [106]. The application is based on the Principal Component Analysis (PCA) concept with a covariance function computed from the training data. The GPMMs start with standard reference shapes such as shown in Fig. 3.

Later, in order to incorporate a specific family of deformations with a dataset, a framework is needed which can assign the probability to all possible deformations for the given input feature. The desired deformations can be modelled by defining a covariance function as shown in Fig. 4.

According to Luthi *et al.* [106] GPMMs come with many advantages over SSMs such as:

- With GPMMs, there is much more freedom in defining the covariance function, by combining different covariance functions (or kernels) to mimic more sophisticated registration schemes. This helps to extend the model beyond the linear span of example data (training data), hence GPMMs work well with little training data.
- GPMMs are generative; therefore, the validity of prior assumptions can be assessed by sampling from the model.
- Shape variations can be well approximated using only a moderate number of leading basis functions (eigenvectors).
- For most anatomical shapes, finely detailed deformations only occur in parts of the shape, and GPMMs give more power to model these slight deformations only where they are needed.
- The above advantages may help in incorporating the medical expert knowledge into the model in order to shape slight deformations.

Hence, GPMMs can be incorporated to deal with the significant and minor deformations that occur on human faces with various subtypes of rosacea (i.e. phymatous rosacea) by creating a 3D model of face with possible deformations from the set of 2D images. GPMMs give us the modelling power to model these fine deformations only where they are needed. This autonomy may help in incorporating medical expert knowledge in order to model slight, local deformations e.g. lesions, enlargement of nose etc. As the effective treatments of rosacea are broadly advancing, a laser and light-based treatment approach to the rosacea diagnosis is recommended [176], [177]. Thus, reconstructing local deformations on the face for specific subtypes of rosacea may help diagnose and support light and laser treatment of the disease condition.

As GPMMs are generative, recently there have been a few applications developed using CNNs and GANs. These models have also succeeded in generating 3D faces [107], [108], [110], [111], [178]–[181]. Therefore, if local deformations of rosacea are successfully generated using GPMMs, then it may help in generating more synthetic datasets of rosacea using a GAN architectures.

VI. DISCUSSION AND OUTLOOK

The majority of the research done in the field of skin disease diagnosis is focused on skin cancer. The lack of publicly available visual data for a skin condition such as rosacea often leads to poor performance in classification and automated diagnosis models. However, the recent advancement in the field of AI and particularly data generation has prompted many opportunities in the future of computer-aided diagnosis for Teledermatology [182] including rosacea.

Although data augmentation and transfer learning have been very successful with medical and clinical image analysis with large datasets, they may not perform as accurately with limited data. Hence, using a classification approach for a limited data problem may not be a good idea at present. However, there is an opportunity to explore techniques to overcome this central problem which may improve the scope of research.

In the field of skin disease analysis, generating synthetic samples that may look as real as certain skin conditions, such as rosacea, can mitigate the problem of data scarcity. As discussed in Section V.B., a few variants of StyleGAN can be

utilised to explore the possibility of generating synthetic faces with rosacea. Nevertheless, the accuracy of the generated data must be examined. For such examinations, it is important to rely on the subjective evaluation methods for image quality, such as the Mean Opinion Score (MOS) of a group of experts.

As discussed in Section V, GANs have a few common limitations, which may lead to unsatisfactory outcomes. Therefore, it is essential to investigate additional methods to deal with limited data without modification, i.e. by keeping the data volume constant and still performing classification. This can be achieved with hyperparameter optimization by adapting the Meta-Learning concept. Nevertheless, meta-learning and few-shot classification are new approaches in medical and clinical image analysis, that offer a solid motivation to explore the techniques. There are a few studies on meta-learning for clinical image analysis, which may provide limited scope for exploration. Further, we discussed 3D modelling as an approach to generate synthetic facial data through GPMMs. By leveraging the concept of GPMMs, unlike GANs, we can handcraft the particular types of appearances on the skin caused by rosacea. This may help identify a few subtypes of rosacea that cause significant deformation on the face.

VII. CONCLUSION AND FUTURE SCOPE

AI and computer vision have performed remarkably well as it approaches understanding and dealing with disease diagnosis using health data. The effectiveness of deep learning has started offering breakthrough outcomes. Nevertheless, there are notable gaps needed to be bridged. Even though the world of AI is running with the concept of big data, it is crucial to draw valid inferences from a small amount of data by wisely tweaking the new information. This is a fundamental challenge in machine learning and computer vision. In this review, to utilise limited availability of skin disease image data, we have investigated a few essential computer vision and machine learning techniques i.e. GANs, meta-learning, few-shot learning, 3D face modelling using GPMMs with important research gaps and noteworthy advantages. It may help navigate future research directions in computer-aided diagnosis for other facial skin conditions when only a small number of clinical images are available for research. Our future work will be aligned with exploring the methodologies of synthetic data generation in details for skin disease analysis such as rosacea as discussed in this paper. The assessment of such technologies can significantly impact the quality of AI and automated examination models to further advance the diagnosis frameworks in the field of dermatology.

REFERENCES

[1] R. J. Hay, N. E. Johns, H. C. Williams, I. W. Bolliger, R. P. Dellavalle, and D. J. Margolis, "The global burden of skin disease in 2010: An analysis of the prevalence and impact of skin conditions," *J. Investigative Dermatol.*, vol. 134, no. 6, pp. 1527–1534, 2014.
[2] D. Seth, K. Cheldize, D. Brown, and E. E. Freeman, "Global burden of skin disease: Inequities and innovations," *Current Dermatol. Rep.*, vol. 6, no. 3, pp. 204–210, Sep. 2017.
[3] C. Flohr and R. Hay, "Putting the burden of skin diseases on the global map," *Brit. J. Dermatol.*, vol. 184, no. 2, pp. 189–190, Feb. 2021.
[4] M. Augustin, M. Reusch, J. Augustin, T. Wagner, and S. Kämpfe. (2013). *European Dermatology Health Care Survey 2013 Short Report*. [Online]. Available: https://www.dermasurvey.eu/wp-content/uploads/eu-derma-health-care-survey-2013-short.pdf
[5] British Association of Dermatologists and The King's Fund. (2014). *How Can Dermatology Services Meet Current and Future Patient Needs, While Ensuring Quality of Care is Not Compromised and Access is Equitable Across the UK?* [Online]. Available: https://www.bad.org.uk/shared/get-file.ashx?id=2347&itemtype=document
[6] Ireland. (2014). *Dermatology Report*. [Online]. Available: https://www.hse.ie/eng/staff/leadership-education-development/met/plan/specialty-specific-reviews/dermatology-2014.pdf
[7] P. R. Mydlarski, L. M. Parsons, T. A. Pierscianowski, M. G. Kirchhof, C. F. Rosen, K. Purdy, J. Powell, S. Humphrey, M. Clermont, S. Elliot, L. Rumleski, and L. Gorman, "Dermatologic training and practice in Canada: An in-depth review," *J. Cutaneous Med. Surg.*, vol. 24, no. 3, pp. 297–303, May 2020.
[8] A. M. Glazer, A. S. Farberg, R. R. Winkelmann, and D. S. Rigel, "Analysis of trends in geographic distribution and density of US dermatologists," *J. Amer. Med. Assoc. Dermatol.*, vol. 153, no. 4, pp. 322–325, 2017.
[9] Australian Government Department of Health. (2016). *Dermatology 2016 Facesheet*. [Online]. Available: https://hwd.health.gov.au/webapi/customer/documents/factsheets/2016/Dermatology.pdf
[10] C.-B. Shen, X. Shen, C.-X. Li, R.-S. Meng, and Y. Cui, "Assessment of imaging diagnosis ability of skin tumors in Chinese dermatologists," *Chin. Med. J.*, vol. 132, no. 17, p. 2119, 2019.
[11] P. Pala, B. S. Bergler-Czop, and J. M. Gwi, "Teledermatology: Idea, benefits and risks of modern age—A systematic review based on melanoma," *Adv. Dermatol. Allergol./Postępy Dermatologii Alergologii*, vol. 37, no. 2, p. 159, 2020.
[12] F. X. Marin-Gomez, J. Vidal-Alaball, P. R. Poch, C. J. Sariola, R. T. Ferrer, and J. M. Peña, "Diagnosis of skin lesions using photographs taken with a mobile phone: An online survey of primary care physicians," *J. Primary Care Community Health*, vol. 11, Jun. 2020, Art. no. 2150132720937831.
[13] NZ Dermatological Society. *Dermnetnz*. Accessed: Oct. 7, 2021. [Online]. Available: https://dermnetnz.org/
[14] F. C. Powell, "Rosacea," *New England J. Med.*, vol. 352, no. 8, pp. 793–803, 2005.
[15] J. Q. D. Rosso, R. L. Gallo, L. Kircik, D. Thiboutot, H. E. Baldwin, and D. Cohen, "Why is rosacea considered to be an inflammatory disorder? The primary role, clinical relevance, and therapeutic correlations of abnormal innate immune response in rosacea-prone skin," *J. Drugs Dermatol.*, vol. 11, no. 6, pp. 694–700, 2012.
[16] M. Steinhoff, J. Schauber, and J. J. Leyden, "New insights into rosacea pathophysiology: A review of recent findings," *J. Amer. Acad. Dermatol.*, vol. 69, no. 6, pp. S15–S26, Dec. 2013.
[17] S. A. Johnston, M. Krasuska, A. Millings, A. C. Lavda, and A. R. Thompson, "Experiences of rosacea and its treatment: An interpretative phenomenological analysis," *Brit. J. Dermatol.*, vol. 178, no. 1, pp. 154–160, Jan. 2018.
[18] P. Hampton, J. Berth-Jones, C. E. D. Williamson, R. Hay, T. A. Leslie, I. Porter, S. Rauz, D. Seukeran, R. T. Winn, M. Hashme, L. S. Exton, M. F. M. Mustapa, and L. Manounah, "British association of dermatologists guidelines for the management of people with rosacea 2021," *Brit. J. Dermatol.*, vol. 185, no. 4, pp. 725–735, 2021.
[19] L. Gether, L. K. Overgaard, A. Egeberg, and J. P. Thyssen, "Incidence and prevalence of rosacea: A systematic review and meta-analysis," *Brit. J. Dermatol.*, vol. 179, no. 2, pp. 282–289, May 2018.
[20] National Rosacea Society. *Red Skin & Rashes are Not Always the Result of Rosacea*. Accessed: Oct. 7, 2021. [Online]. Available: https://www.rosacea.org/blog/2016/june/red-skin-rashes-are-not-always-the-result-of-rosacea
[21] Acne and Rosacea Society of Canada. *The National Rosacea Society has Conducted Surveys of Rosacea Sufferers to Offer Insights Into the Effect on Social Life*. Accessed: Oct. 7, 2021. [Online]. Available: https://www.rosaceahelp.ca/impact/social-life/
[22] J. Spoendlin, J. J. Voegel, S. S. Jick, and C. R. Meier, "A study on the epidemiology of rosacea in the U.K.," *Brit. J. Dermatol.*, vol. 167, no. 3, pp. 598–605, 2012.
[23] Acne and Rosacea Society of Canada. *Rosacea Affects More Than 3 Million Canadians*. Accessed: Oct. 7, 2021. [Online]. Available: https://www.rosaceahelp.ca/
[24] M. Berg and S. Lidén, "Postmenopausal female rosacea patients are more disposed to react with migraine," *Dermatology*, vol. 193, no. 1, pp. 73–74, 1996.

[25] Grand View Research. (2019). *Rosacea Treatment Market Size, Share & Trends Analysis Report by Drug Class (Alpha Agonists, Antibiotics, Retinoids, Corticosteroids), by Mode of Administration (Topical, Oral), by Region, and Segment Forecasts, 2019–2025, Report ID: GVR-2-68038-739-1*. [Online]. Available: https://www.grandviewresearch.com/industry-analysis/rosacea-treatment-market

[26] Dermatology Times. (2021). *2021 Rosacea Report*. [Online]. Available: https://www.dermatologytimes.com/view/top-20-trending-stories-of-2020

[27] USNewsHealth. (2021). *Treatments for Rosacea*. [Online]. Available: https://health.usnews.com/health-care/patient-advice/articles/treatments-for-rosacea

[28] TheIrishTimes. (2021). *Rosacea: What is it and How Can You Manage it?* [Online]. Available: https://www.irishtimes.com/life-and-style/fashion/beauty/rosacea-what-is-it-and-how-can-you-manage-it-1.4575944

[29] A. Esteva, B. Kuprel, R. A. Novoa, J. Ko, S. M. Swetter, H. M. Blau, and S. Thrun, "Dermatologist-level classification of skin cancer with deep neural networks," *Nature*, vol. 542, no. 7639, pp. 115–118, 2017.

[30] Y. LeCun, Y. Bengio, and G. E. Hinton, "Deep learning," *Nature*, vol. 521, no. 7553, pp. 436–444, Dec. 2015.

[31] K. Thomsen, A. L. Christensen, L. Iversen, H. B. Lomholt, and O. Winther, "Deep learning for diagnostic binary classification of multiple-lesion skin diseases," *Frontiers Med.*, vol. 7, p. 604, Sep. 2020.

[32] Z. Zhao, C.-M. Wu, S. Zhang, F. He, F. Liu, B. Wang, Y. Huang, W. Shi, D. Jian, H. Xie, C.-Y. Yeh, and J. Li, "A novel convolutional neural network for the diagnosis and classification of rosacea: Usability study," *JMIR Med. Informat.*, vol. 9, no. 3, Mar. 2021, Art. no. e23415.

[33] H. Wu *et al.*, "A deep learning, image based approach for automated diagnosis for inflammatory skin diseases," *Ann. Transl. Med.*, vol. 8, no. 9, p. 581, May 2020.

[34] C.-Y. Zhu, Y.-K. Wang, H.-P. Chen, K.-L. Gao, C. Shu, J.-C. Wang, L.-F. Yan, Y.-G. Yang, F.-Y. Xie, and J. Liu, "A deep learning based framework for diagnosing multiple skin diseases in a clinical environment," *Frontiers Med.*, vol. 8, Apr. 2021, Art. no. 626369.

[35] J. Deng, W. Dong, R. Socher, L.-J. Li, K. Li, and L. Fei-Fei, "ImageNet: A large-scale hierarchical image database," in *Proc. IEEE Conf. Comput. Vis. Pattern Recognit.*, Jun. 2009, pp. 248–255.

[36] E. Goceri, "Diagnosis of skin diseases in the era of deep learning and mobile technology," *Comput. Biol. Med.*, vol. 134, Jul. 2021, Art. no. 104458.

[37] A. G. Howard, M. Zhu, B. Chen, D. Kalenichenko, W. Wang, T. Weyand, M. Andreetto, and H. Adam, "MobileNets: Efficient convolutional neural networks for mobile vision applications," 2017, *arXiv:1704.04861*.

[38] K. Simonyan and A. Zisserman, "Very deep convolutional networks for large-scale image recognition," 2014, *arXiv:1409.1556*.

[39] E. Goceri, "Deep learning based classification of facial dermatological disorders," *Comput. Biol. Med.*, vol. 128, Jan. 2021, Art. no. 104118.

[40] G. Huang, Z. Liu, L. Van Der Maaten, and K. Q. Weinberger, "Densely connected convolutional networks," in *Proc. IEEE Conf. Comput. Vis. Pattern Recognit. (CVPR)*, Jul. 2017, pp. 4700–4708.

[41] C. Szegedy, S. Ioffe, V. Vanhoucke, and A. A. Alemi, "Inception-v4, inception-ResNet and the impact of residual connections on learning," in *Proc. 31st AAAI Conf. Artif. Intell.*, 2017, pp. 1–7.

[42] M. Tan and Q. Le, "EfficientNet: Rethinking model scaling for convolutional neural networks," in *Proc. Int. Conf. Mach. Learn.*, 2019, pp. 6105–6114.

[43] C. Szegedy, V. Vanhoucke, S. Ioffe, J. Shlens, and Z. Wojna, "Rethinking the inception architecture for computer vision," in *Proc. IEEE Conf. Comput. Vis. Pattern Recognit. (CVPR)*, Jun. 2016, pp. 2818–2826.

[44] K. He, X. Zhang, S. Ren, and J. Sun, "Deep residual learning for image recognition," in *Proc. IEEE Conf. Comput. Vis. Pattern Recognit. (CVPR)*, Jun. 2016, pp. 770–778.

[45] S. L. P. Aggarwal, "Data augmentation in dermatology image recognition using machine learning," *Skin Res. Technol.*, vol. 25, no. 6, pp. 815–820, Nov. 2019.

[46] H. Binol, A. Plotner, J. Sopkovich, B. Kaffenberger, M. K. K. Niazi, and M. N. Gurcan, "Ros-NET: A deep convolutional neural network for automatic identification of rosacea lesions," *Skin Res. Technol.*, vol. 26, no. 3, pp. 413–421, May 2020.

[47] B. Xie, X. He, S. Zhao, Y. Li, J. Su, X. Zhao, Y. Kuang, Y. Wang, and X. Chen, "XiangyaDerm: A clinical image dataset of Asian race for skin disease aided diagnosis," in *Large-Scale Annotation of Biomedical Data and Expert Label Synthesis and Hardware Aware Learning for Medical Imaging and Computer Assisted Intervention*. Cham, Switzerland: Springer, 2019, pp. 22–31.

[48] F. Chollet, "Xception: Deep learning with depthwise separable convolutions," in *Proc. IEEE Conf. Comput. Vis. Pattern Recognit. (CVPR)*, Jul. 2017, pp. 1251–1258.

[49] Y. LeCun. (1998). *The MNIST Database of Handwritten Digits*. [Online]. Available: http://yann.lecun.com/exdb/mnist/

[50] Y. LeCun, L. Bottou, Y. Bengio, and P. Haffner, "Gradient-based learning applied to document recognition," *Proc. IEEE*, vol. 86, no. 11, pp. 2278–2324, Nov. 1998.

[51] D. S. W. Ting and *et al.*, "Development and validation of a deep learning system for diabetic retinopathy and related eye diseases using retinal images from multiethnic populations with diabetes," *J. Amer. Med. Assoc.*, vol. 318, no. 22, pp. 2211–2223, 2017.

[52] R. Lindsey, "Deep neural network improves fracture detection by clinicians," *Proc. Nat. Acad. Sci. USA*, vol. 115, no. 45, pp. 11591–11596, 2018.

[53] Y. Peng, S. Dharssi, Q. Chen, T. D. Keenan, E. Agrón, W. T. Wong, E. Y. Chew, and Z. Lu, "DeepSeeNet: A deep learning model for automated classification of patient-based age-related macular degeneration severity from color fundus photographs," *Ophthalmology*, vol. 126, no. 4, pp. 565–575, Apr. 2019.

[54] O. Bernard *et al.*, "Deep learning techniques for automatic MRI cardiac multi-structures segmentation and diagnosis: Is the problem solved?" *IEEE Trans. Med. Imag.*, vol. 37, no. 11, pp. 2514–2525, Nov. 2018.

[55] A. R. Feyjie, R. Azad, M. Pedersoli, C. Kauffman, I. B. Ayed, and J. Dolz, "Semi-supervised few-shot learning for medical image segmentation," 2020, *arXiv:2003.08462*.

[56] Z. Zhao, B. Liu, Y. Guo, and J. Ye, "Ensemble model with batch spectral regularization and data blending for cross-domain few-shot learning with unlabeled data," 2020, *arXiv:2006.04323*.

[57] R. Miotto, F. Wang, S. Wang, X. Jiang, and J. T. Dudley, "Deep learning for healthcare: Review, opportunities and challenges," *Briefings Bioinf.*, vol. 19, no. 6, pp. 1236–1246, 2018.

[58] J. M. Johnson and T. M. Khoshgoftaar, "Survey on deep learning with class imbalance," *J. Big Data*, vol. 6, no. 1, pp. 1–54, Dec. 2019.

[59] Z. Li, K. Kamnitsas, and B. Glocker, "Overfitting of neural nets under class imbalance: Analysis and improvements for segmentation," in *Proc. Int. Conf. Med. Image Comput. Comput.-Assist. Intervent.* Cham, Switzerland: Springer, 2019, pp. 402–410.

[60] J. Kawahara, S. Daneshvar, G. Argenziano, and G. Hamarneh, "Seven-point checklist and skin lesion classification using multitask multimodal neural nets," *IEEE J. Biomed. Health Informat.*, vol. 23, no. 2, pp. 538–546, Mar. 2019.

[61] S. S. Han, M. S. Kim, W. Lim, G. H. Park, I. Park, and S. E. Chang, "Classification of the clinical images for benign and malignant cutaneous tumors using a deep learning algorithm," *J. Investigative Dermatol.*, vol. 138, no. 7, pp. 1529–1538, 2018.

[62] *Dermatology Atlas Brazil*. Accessed: Nov. 3, 2021. [Online]. Available: http://www.atlasdermatologico.com.br/index.jsf

[63] An Atlas of Clinical Dermatology Denmark. *An Atlas of Clinical Dermatology*. Accessed: Nov. 3, 2021. [Online]. Available: https://danderm.dk/atlas/index.html

[64] *DermIS*. Accessed: Nov. 3, 2021. [Online]. Available: https://www.dermis.net/dermisroot/en/home/index.htm

[65] *DermNet Skin Disease Atlas*. Accessed: Nov. 3, 2021. [Online]. Available: http://www.dermnet.com

[66] The University of Edinburgh. *Dermofit Image Library*. Accessed: Nov. 3, 2021. [Online]. Available: https://licensing.edinburgh-innovations.ed.ac.uk/i/softwaredermofit-image-library.html

[67] *Dermato Web Spain*. Accessed: Nov. 3, 2021. [Online]. Available: http://dermatoweb.net

[68] P. Tschandl, C. Rosendahl, and H. Kittler, "The HAM10000 dataset, a large collection of multi-source dermatoscopic images of common pigmented skin lesions," *Sci. Data*, vol. 5, no. 1, pp. 1–9, Dec. 2018.

[69] *Hellenic Dermatological Atlas*. Accessed: Nov. 3, 2021. [Online]. Available: http://www.hellenicdermatlas.com/en/

[70] V. Rotemberg *et al.*, "A patient-centric dataset of images and metadata for identifying melanomas using clinical context," *Sci. Data*, vol. 8, no. 1, pp. 1–8, Dec. 2021.

[71] *ISIC Archive*. Accessed: Nov. 3, 2021. [Online]. Available: https://www.isic-archive.com

[72] I. Giotis, N. Molders, S. Land, M. Biehl, M. F. Jonkman, and N. Petkov, "MED-NODE: A computer-assisted melanoma diagnosis system using non-dermoscopic images," *Expert Syst. Appl.*, vol. 42, no. 19, pp. 6578–6585, Nov. 2015.

[73] *Molemap NewZealand*. Accessed: Nov. 6, 2021. [Online]. Available: https://www.molemap.co.nz
[74] Z. Ge, S. Demyanov, B. Bozorgtabar, M. Abedini, R. Chakravorty, A. Bowling, and R. Garnavi, "Exploiting local and generic features for accurate skin lesions classification using clinical and dermoscopy imaging," in *Proc. IEEE 14th Int. Symp. Biomed. Imag. (ISBI)*, Apr. 2017, pp. 986–990.
[75] T. Mendonça, P. M. Ferreira, J. S. Marques, A. R. Marcal, and J. Rozeira, "PH^2—A dermoscopic image database for research and benchmarking," in *Proc. 35th Annu. Int. Conf. IEEE Eng. Med. Biol. Soc. (EMBC)*, Jul. 2013, pp. 5437–5440.
[76] X. Sun, J. Yang, M. Sun, and K. Wang, "A benchmark for automatic visual classification of clinical skin disease images," in *Proc. Eur. Conf. Comput. Vis.* Berlin, Germany: Springer, 2016, pp. 206–222.
[77] *SD198*. Accessed: Nov. 6, 2021. [Online]. Available: http://xiaopingwu.cn/assets/projects/sd-198/
[78] A. Masood and A. A. Al-Jumaily, "Computer aided diagnostic support system for skin cancer: A review of techniques and algorithms," *Int. J. Biomed. Imag.*, vol. 2013, pp. 1–22, Oct. 2013.
[79] B. Rosado, S. Menzies, A. Harbauer, H. Pehamberger, K. Wolff, M. Binder, and H. Kittler, "Accuracy of computer diagnosis of melanoma: A quantitative meta-analysis," *Arch. Dermatol.*, vol. 139, no. 3, pp. 361–367, 2003.
[80] M. Burroni, R. Corona, G. Dell'Eva, F. Sera, R. Bono, P. Puddu, R. Perotti, F. Nobile, L. Andreassi, and P. Rubegni, "Melanoma computer-aided diagnosis: Reliability and feasibility study," *Clin. Cancer Res.*, vol. 10, no. 6, pp. 1881–1886, Mar. 2004.
[81] H. Kittler, H. Pehamberger, K. Wolff, and M. Binder, "Diagnostic accuracy of dermoscopy," *Lancet Oncol.*, vol. 3, no. 3, pp. 159–165, Mar. 2002.
[82] D. Gutman, N. C. F. Codella, E. Celebi, B. Helba, M. Marchetti, N. Mishra, and A. Halpern, "Skin lesion analysis toward melanoma detection: A challenge at the international symposium on biomedical imaging (ISBI) 2016, hosted by the international skin imaging collaboration (ISIC)," 2016, *arXiv:1605.01397*.
[83] M. Binder, H. Kittler, A. Seeber, A. Steiner, H. Pehamberger, and K. Wolff, "Epiluminescence microscopy-based classification of pigmented skin lesions using computerized image analysis and an artificial neural network," *Melanoma Res.*, vol. 8, no. 3, pp. 261–266, Jun. 1998.
[84] S.-I. Amari *et al.*, *The Handbook of Brain Theory and Neural Networks*. Cambridge, MA, USA: MIT Press, 2003.
[85] B. Erickson, P. Korfiatis, Z. Akkus, and T. Kline, "Machine learning for medical imaging," *RadioGraphics*, vol. 37, no. 2, pp. 505–515, 2017.
[86] H. Greenspan, B. Van Ginneken, and R. M. Summers, "Guest editorial deep learning in medical imaging: Overview and future promise of an exciting new technique," *IEEE Trans. Med. Imag.*, vol. 35, no. 5, pp. 1153–1159, May 2016.
[87] M. L. Giger, "Machine learning in medical imaging," *J. Amer. College Radiol.*, vol. 15, no. 3, pp. 512–520, Mar. 2018.
[88] J. G. Lee, S. Jun, Y.-W. Cho, H. Lee, G. B. Kim, J. B. Seo, and N. Kim, "Deep learning in medical imaging: General overview," *Korean J. Radiol.*, vol. 18, no. 4, pp. 570–584, 2017.
[89] K. Suzuki, "Overview of deep learning in medical imaging," *Radiol. Phys. Technol.*, vol. 10, no. 3, pp. 257–273, 2017.
[90] I. Goodfellow, Y. Bengio, and A. Courville, *Deep Learning*. Cambridge, MA, USA: MIT Press, 2016.
[91] A. Krizhevsky, I. Sutskever, and G. E. Hinton, "ImageNet classification with deep convolutional neural networks," in *Proc. Adv. Neural Inf. Process. Syst.*, vol. 25, 2012, pp. 1097–1105.
[92] O. Russakovsky, J. Deng, H. Su, J. Krause, S. Satheesh, S. Ma, Z. Huang, A. Karpathy, A. Khosla, M. Bernstein, A. C. Berg, and L. Fei-Fei, "ImageNet large scale visual recognition challenge," *Int. J. Comput. Vis.*, vol. 115, no. 3, pp. 211–252, 2015.
[93] N. Papernot, P. McDaniel, S. Jha, M. Fredrikson, Z. B. Celik, and A. Swami, "The limitations of deep learning in adversarial settings," in *Proc. IEEE Eur. Symp. Secur. Privacy (EuroSP)*, Mar. 2016, pp. 372–387.
[94] I. Goodfellow, "NIPS 2016 tutorial: Generative adversarial networks," 2017, *arXiv:1701.00160*.
[95] I. Goodfellow, J. Pouget-Abadie, M. Mirza, B. Xu, D. Warde-Farley, S. Ozair, A. Courville, and Y. Bengio, "Generative adversarial nets," in *Proc. Adv. Neural Inf. Process. Syst.*, vol. 27, 2014, pp. 1–9.
[96] L. Lan, L. You, Z. Zhang, Z. Fan, W. Zhao, N. Zeng, Y. Chen, and X. Zhou, "Generative adversarial networks and its applications in biomedical informatics," *Frontiers Public Health*, vol. 8, p. 164, May 2020.
[97] S. Kazeminia, C. Baur, A. Kuijper, B. van Ginneken, N. Navab, S. Albarqouni, and A. Mukhopadhyay, "GANs for medical image analysis," *Artif. Intell. Med.*, vol. 109, Sep. 2020, Art. no. 101938.
[98] L. Weng. (2018). *Meta-Learning: Learning to Learn Fast*. [Online]. Available: https://lilianweng.github.io/lil-log/2018/11/30/meta-learning.html
[99] C. B. Finn, *Learning to Learn With Gradients*. Berkeley, CA, USA: Univ. of California, Berkeley, 2018.
[100] C. Finn, P. Abbeel, and S. Levine, "Model-agnostic meta-learning for fast adaptation of deep networks," in *Proc. Int. Conf. Mach. Learn.*, 2017, pp. 1126–1135.
[101] V. Blanz and T. Vetter, "A morphable model for the synthesis of 3D faces," in *Proc. 26th Annu. Conf. Comput. Graph. Interact. Techn.*, 1999, pp. 187–194.
[102] B. Egger, W. A. P. Smith, A. Tewari, S. Wuhrer, M. Zollhoefer, T. Beeler, F. Bernard, T. Bolkart, A. Kortylewski, S. Romdhani, C. Theobalt, V. Blanz, and T. Vetter, "3D morphable face models—Past, present, and future," *ACM Trans. Graph.*, vol. 39, no. 5, pp. 1–38, 2020.
[103] T. Cootes, E. Baldock, and J. Graham, "An introduction to active shape models," in *Image Processing and Analysis*, vol. 328. Oxford, U.K.: Oxford Univ. Press, 2000, pp. 223–248.
[104] T. F. Cootes and C. J. Taylor, "Statistical models of appearance for medical image analysis and computer vision," *Proc. SPIE*, vol. 4322, pp. 236–248, Jul. 2001.
[105] D. Cristinacce and T. F. Cootes, "Boosted regression active shape models," in *Proc. BMVC*, vol. 2. Princeton, NJ, USA: Citeseer, 2007, pp. 880–889.
[106] M. Lüthi, T. Gerig, C. Jud, and T. Vetter, "Gaussian process morphable models," *IEEE Trans. Pattern Anal. Mach. Intell.*, vol. 40, no. 8, pp. 1860–1873, Aug. 2018.
[107] A. S. Jackson, A. Bulat, V. Argyriou, and G. Tzimiropoulos, "Large pose 3D face reconstruction from a single image via direct volumetric CNN regression," in *Proc. IEEE Int. Conf. Comput. Vis. (ICCV)*, Oct. 2017, pp. 1031–1039.
[108] A. T. Tran, T. Hassner, I. Masi, and G. Medioni, "Regressing robust and discriminative 3D morphable models with a very deep neural network," in *Proc. IEEE Conf. Comput. Vis. Pattern Recognit. (CVPR)*, Jul. 2017, pp. 5163–5172.
[109] X.-F. Han, H. Laga, and M. Bennamoun, "Image-based 3D object reconstruction: State-of-the-art and trends in the deep learning era," *IEEE Trans. Pattern Anal. Mach. Intell.*, vol. 43, no. 5, pp. 1578–1604, May 2021.
[110] B. Gecer, S. Ploumpis, I. Kotsia, and S. Zafeiriou, "GANFIT: Generative adversarial network fitting for high fidelity 3D face reconstruction," in *Proc. IEEE/CVF Conf. Comput. Vis. Pattern Recognit. (CVPR)*, Jun. 2019, pp. 1155–1164.
[111] J. Song, J. Zhang, L. Gao, Z. Zhao, and H. T. Shen, "AgeGAN++: Face aging and rejuvenation with dual conditional GANs," *IEEE Trans. Multimedia*, vol. 24, pp. 791–804, 2022.
[112] C. Shorten and T. M. Khoshgoftaar, "A survey on image data augmentation for deep learning," *J. Big Data*, vol. 6, no. 1, pp. 1–48, Dec. 2019.
[113] S. J. Pan and Q. Yang, "A survey on transfer learning," *IEEE Trans. Knowl. Data Eng.*, vol. 22, no. 10, pp. 1345–1359, Oct. 2010.
[114] Y. Liu, A. Jain, C. Eng, D. H. Way, K. Lee, P. Bui, K. Kanada, G. de Oliveira Marinho, J. Gallegos, S. Gabriele, and V. Gupta, "A deep learning system for differential diagnosis of skin diseases," *Nature Med.*, vol. 26, no. 6, pp. 900–908, 2020.
[115] E. Goceri, "Skin disease diagnosis from photographs using deep learning," in *Proc. ECCOMAS Thematic Conf. Comput. Vis. Med. Image Process.* Cham, Switzerland: Springer, 2019, pp. 239–246.
[116] M. A. A. Milton, "Automated skin lesion classification using ensemble of deep neural networks in ISIC 2018: Skin lesion analysis towards melanoma detection challenge," 2019, *arXiv:1901.10802*.
[117] X. Cui, R. Wei, L. Gong, R. Qi, Z. Zhao, H. Chen, K. Song, A. A. A. Abdulrahman, Y. Wang, J. Z. S. Chen, S. Chen, Y. Zhao, and X. Gao, "Assessing the effectiveness of artificial intelligence methods for melanoma: A retrospective review," *J. Amer. Acad. Dermatol.*, vol. 81, no. 5, pp. 1176–1180, Nov. 2019.
[118] C. Yu, S. Yang, W. Kim, J. Jung, K.-Y. Chung, S. W. Lee, and B. Oh, "Acral melanoma detection using a convolutional neural network for dermoscopy images," *PLoS ONE*, vol. 13, no. 3, Mar. 2018, Art. no. e0193321.

[119] A. Kwasigroch, A. Mikołajczyk, and M. Grochowski, "Deep neural networks approach to skin lesions classification—A comparative analysis," in *Proc. 22nd Int. Conf. Methods Models Autom. Robot. (MMAR)*, Aug. 2017, pp. 1069–1074.

[120] A. Romero-Lopez, X. Giro-i-Nieto, J. Burdick, and O. Marques, "Skin lesion classification from dermoscopic images using deep learning techniques," in *Proc. 13th IASTED Int. Conf. Biomed. Eng. (BioMed)*, 2017, pp. 49–54.

[121] S. H. Kassani and P. H. Kassani, "A comparative study of deep learning architectures on melanoma detection," *Tissue Cell*, vol. 58, pp. 76–83, Jun. 2019.

[122] M. A. Morid, A. Borjali, and G. Del Fiol, "A scoping review of transfer learning research on medical image analysis using ImageNet," *Comput. Biol. Med.*, vol. 128, Jan. 2021, Art. no. 104115.

[123] Z. Wang, Z. Dai, B. Póczos, and J. Carbonell, "Characterizing and avoiding negative transfer," in *Proc. IEEE/CVF Conf. Comput. Vis. Pattern Recognit. (CVPR)*, Jun. 2019, pp. 11293–11302.

[124] S. Mishra, T. Yamasaki, and H. Imaizumi, "Supervised classification of dermatological diseases by deep learning," 2018, *arXiv:1802.03752*.

[125] J. Yang, X. Sun, J. Liang, and P. L. Rosin, "Clinical skin lesion diagnosis using representations inspired by dermatologist criteria," in *Proc. IEEE/CVF Conf. Comput. Vis. Pattern Recognit.*, Jun. 2018, pp. 1258–1266.

[126] W. Sae-Lim, W. Wettayaprasit, and P. Aiyarak, "Convolutional neural networks using MobileNet for skin lesion classification," in *Proc. 16th Int. Joint Conf. Comput. Sci. Softw. Eng. (JCSSE)*, Jul. 2019, pp. 242–247.

[127] K. Polat and K. O. Koc, "Detection of skin diseases from dermoscopy image using the combination of convolutional neural network and one-versus-all," *J. Artif. Intell. Syst.*, vol. 2, no. 1, pp. 80–97, 2020.

[128] K. M. Hosny, M. A. Kassem, and M. M. Foaud, "Classification of skin lesions using transfer learning and augmentation with Alex-Net," *PLoS ONE*, vol. 14, no. 5, May 2019, Art. no. e0217293.

[129] A. Mahbod, G. Schaefer, C. Wang, R. Ecker, and I. Ellinge, "Skin lesion classification using hybrid deep neural networks," in *Proc. IEEE Int. Conf. Acoust., Speech Signal Process. (ICASSP)*, May 2019, pp. 1229–1233.

[130] D. B. Mendes and N. C. da Silva, "Skin lesions classification using convolutional neural networks in clinical images," 2018, *arXiv:1812.02316*.

[131] Z. Qin, Z. Liu, P. Zhu, and Y. Xue, "A GAN-based image synthesis method for skin lesion classification," *Comput. Methods Programs Biomed.*, vol. 195, Oct. 2020, Art. no. 105568.

[132] H. Rashid, M. A. Tanveer, and H. A. Khan, "Skin lesion classification using GAN based data augmentation," in *Proc. 41st Annu. Int. Conf. IEEE Eng. Med. Biol. Soc. (EMBC)*, Jul. 2019, pp. 916–919.

[133] A. Radford, L. Metz, and S. Chintala, "Unsupervised representation learning with deep convolutional generative adversarial networks," 2015, *arXiv:1511.06434*.

[134] E. Denton, S. Chintala, A. Szlam, and R. Fergus, "Deep generative image models using a Laplacian pyramid of adversarial networks," 2015, *arXiv:1506.05751*.

[135] M. Mirza and S. Osindero, "Conditional generative adversarial nets," 2014, *arXiv:1411.1784*.

[136] T. Karras, T. Aila, S. Laine, and J. Lehtinen, "Progressive growing of GANs for improved quality, stability, and variation," 2017, *arXiv:1710.10196*.

[137] C. Baur, S. Albarqouni, and N. Navab, "MelanoGANs: High resolution skin lesion synthesis with GANs," 2018, *arXiv:1804.04338*.

[138] C. Baur, S. Albarqouni, and N. Navab, "Generating highly realistic images of skin lesions with GANs," in *OR 2.0 Context-Aware Operating Theaters, Computer Assisted Robotic Endoscopy, Clinical Image-Based Procedures, and Skin Image Analysis*. Cham, Switzerland: Springer, 2018, pp. 260–267.

[139] B. Lei, Z. Xia, F. Jiang, X. Jiang, Z. Ge, Y. Xu, J. Qin, S. Chen, T. Wang, and S. Wang, "Skin lesion segmentation via generative adversarial networks with dual discriminators," *Med. Image Anal.*, vol. 64, Aug. 2020, Art. no. 101716.

[140] D. Bisla, A. Choromanska, R. S. Berman, J. A. Stein, and D. Polsky, "Towards automated melanoma detection with deep learning: Data purification and augmentation," in *Proc. IEEE/CVF Conf. Comput. Vis. Pattern Recognit. Workshops (CVPRW)*, Jun. 2019, pp. 1–9.

[141] A. Bissoto, F. Perez, E. Valle, and S. Avila, "Skin lesion synthesis with generative adversarial networks," in *OR 2.0 Context-Aware Operating Theaters, Computer Assisted Robotic Endoscopy, Clinical Image-Based Procedures, and Skin Image Analysis*. Cham, Switzerland: Springer, 2018, pp. 294–302.

[142] F. Pollastri, F. Bolelli, R. Paredes, and C. Grana, "Augmenting data with GANs to segment melanoma skin lesions," *Multimedia Tools Appl.*, vol. 79, nos. 21–22, pp. 15575–15592, Jun. 2020.

[143] A. Ghorbani, V. Natarajan, D. Coz, and Y. Liu, "DermGAN: Synthetic generation of clinical skin images with pathology," in *Proc. Mach. Learn. Health Workshop*, 2020, pp. 155–170.

[144] S. Fossen-Romsaas, A. Storm-Johannessen, and A. S. Lundervold, "Synthesizing skin lesion images using CycleGANs—A case study," in *Proc. Norsk IKT-Konferanse Forskning Utdanning*, 2020, no. 1.

[145] A. Bissoto, E. Valle, and S. Avila, "GAN-based data augmentation and anonymization for skin-lesion analysis: A critical review," in *Proc. IEEE/CVF Conf. Comput. Vis. Pattern Recognit. Workshops (CVPRW)*, Jun. 2021, pp. 1847–1856.

[146] T. Karras, S. Laine, and T. Aila, "A style-based generator architecture for generative adversarial networks," in *Proc. IEEE/CVF Conf. Comput. Vis. Pattern Recognit. (CVPR)*, Jun. 2019, pp. 4401–4410.

[147] T. Karras, S. Laine, M. Aittala, J. Hellsten, J. Lehtinen, and T. Aila, "Analyzing and improving the image quality of StyleGAN," in *Proc. IEEE/CVF Conf. Comput. Vis. Pattern Recognit. (CVPR)*, Jun. 2020, pp. 8110–8119.

[148] T.-C. Wang, M.-Y. Liu, J.-Y. Zhu, A. Tao, J. Kautz, and B. Catanzaro, "High-resolution image synthesis and semantic manipulation with conditional GANs," in *Proc. IEEE/CVF Conf. Comput. Vis. Pattern Recognit.*, Jun. 2018, pp. 8798–8807.

[149] T. Park, M.-Y. Liu, T.-C. Wang, and J.-Y. Zhu, "Semantic image synthesis with spatially-adaptive normalization," in *Proc. IEEE/CVF Conf. Comput. Vis. Pattern Recognit. (CVPR)*, Jun. 2019, pp. 2337–2346.

[150] L. Chai, J. Wulff, and P. Isola, "Using latent space regression to analyze and leverage compositionality in GANs," 2021, *arXiv:2103.10426*.

[151] T. Karras, M. Aittala, J. Hellsten, S. Laine, J. Lehtinen, and T. Aila, "Training generative adversarial networks with limited data," 2020, *arXiv:2006.06676*.

[152] T. Munkhdalai and H. Yu, "Meta networks," in *Proc. Int. Conf. Mach. Learn.*, 2017, pp. 2554–2563.

[153] A. Santoro, S. Bartunov, M. Botvinick, D. Wierstra, and T. Lillicrap, "Meta-learning with memory-augmented neural networks," in *Proc. Int. Conf. Mach. Learn.*, 2016, pp. 1842–1850.

[154] N. Mishra, M. Rohaninejad, X. Chen, and P. Abbeel, "A simple neural attentive meta-learner," 2017, *arXiv:1707.03141*.

[155] O. Vinyals, C. Blundell, T. Lillicrap, K. Kavukcuoglu, and D. Wierstra, "Matching networks for one shot learning," in *Proc. Adv. Neural Inf. Process. Syst.*, vol. 29, 2016, pp. 3630–3638.

[156] F. Sung, Y. Yang, L. Zhang, T. Xiang, P. H. S. Torr, and T. M. Hospedales, "Learning to compare: Relation network for few-shot learning," in *Proc. IEEE/CVF Conf. Comput. Vis. Pattern Recognit.*, Jun. 2018, pp. 1199–1208.

[157] V. Garcia and J. Bruna, "Few-shot learning with graph neural networks," 2017, *arXiv:1711.04043*.

[158] J. Snell, K. Swersky, and R. S. Zemel, "Prototypical networks for few-shot learning," 2017, *arXiv:1703.05175*.

[159] A. Nichol, J. Achiam, and J. Schulman, "On first-order meta-learning algorithms," 2018, *arXiv:1803.02999*.

[160] J. Kim, S. Lee, S. Kim, M. Cha, J. K. Lee, Y. Choi, Y. Choi, D.-Y. Cho, and J. Kim, "Auto-meta: Automated gradient based meta learner search," 2018, *arXiv:1806.06927*.

[161] E. Grefenstette, B. Amos, D. Yarats, P. M. Htut, A. Molchanov, F. Meier, D. Kiela, K. Cho, and S. Chintala, "Generalized inner loop meta-learning," 2019, *arXiv:1910.01727*.

[162] S. Baik, M. Choi, J. Choi, H. Kim, and K. M. Lee, "Meta-learning with adaptive hyperparameters," 2020, *arXiv:2011.00209*.

[163] A. Zhao, G. Balakrishnan, F. Durand, J. V. Guttag, and A. V. Dalca, "Data augmentation using learned transforms for one-shot medical image segmentation," *CoRR*, vol. abs/1902.09383, pp. 8535–8545, Jun. 2019.

[164] Y. Guo, N. C. Codella, L. Karlinsky, J. V. Codella, J. R. Smith, K. Saenko, T. Rosing, and R. Feris, "A broader study of cross-domain few-shot learning," in *Proc. Eur. Conf. Comput. Vis.* Cham, Switzerland: Springer, 2020, pp. 124–141.

[165] M. Patacchiola, J. Turner, E. J. Crowley, M. O'Boyle, and A. Storkey, "Bayesian meta-learning for the few-shot setting via deep kernels," 2019, *arXiv:1910.05199*.

[166] J. Cai, B. Cai, and S. M. Shen, "SB-MTL: Score-based meta transfer-learning for cross-domain few-shot learning," 2020, *arXiv:2012.01784*.

[167] Q. Sun, Y. Liu, T.-S. Chua, and B. Schiele, "Meta-transfer learning for few-shot learning," in *Proc. IEEE/CVF Conf. Comput. Vis. Pattern Recognit. (CVPR)*, Jun. 2019, pp. 403–412.

[168] S. Gidaris, A. Bursuc, N. Komodakis, P. P. Pérez, and M. Cord, "Boosting few-shot visual learning with self-supervision," in *Proc. IEEE/CVF Int. Conf. Comput. Vis. (ICCV)*, Oct. 2019, pp. 8059–8068.
[169] T. Hospedales, A. Antoniou, P. Micaelli, and A. Storkey, "Meta-learning in neural networks: A survey," 2020, *arXiv:2004.05439*.
[170] Y. Wang, Q. Yao, J. T. Kwok, and L. M. Ni, "Generalizing from a few examples: A survey on few-shot learning," *ACM Comput. Surv.*, vol. 53, no. 3, pp. 1–34, 2020.
[171] X. Li, L. Yu, Y. Jin, C.-W. Fu, L. Xing, and P.-A. Heng, "Difficulty-aware meta-learning for rare disease diagnosis," in *Proc. Int. Conf. Med. Image Comput. Comput.-Assist. Intervent.* Cham, Switzerland: Springer, 2020, pp. 357–366.
[172] K. Mahajan, M. Sharma, and L. Vig, "Meta-DermDiagnosis: Few-shot skin disease identification using meta-learning," in *Proc. IEEE/CVF Conf. Comput. Vis. Pattern Recognit. Workshops (CVPRW)*, Jun. 2020, pp. 730–731.
[173] D. Zhang, M. Jin, and P. Cao, "ST-MetaDiagnosis: Meta learning with spatial transform for rare skin disease diagnosis," in *Proc. IEEE Int. Conf. Bioinf. Biomed. (BIBM)*, Dec. 2020, pp. 2153–2160.
[174] U. Grenander and M. I. Miller, *Pattern Theory: From Representation to Inference*. London, U.K.: Oxford Univ. Press, 2006.
[175] T. Gerig, "Gaussian process morphable models for spatially-varying multi-scale registration," Ph.D. dissertation, Dept. Math. Comput. Sci., Univ. Basel, Basel, Switzerland, 2021.
[176] H. Zhang, K. Tang, Y. Wang, R. Fang, and Q. Sun, "Rosacea treatment: Review and update," *Dermatol. Therapy*, vol. 11, no. 1, pp. 13–24, 2021.
[177] H. Husein-ElAhmed and M. Steinhoff, "Laser and light-based therapies in the management of rosacea: An updated systematic review," *Lasers Med. Sci.*, vol. 36, pp. 1151–1160, Jan. 2021.
[178] K. Genova, F. Cole, A. Maschinot, A. Sarna, D. Vlasic, and W. T. Freeman, "Unsupervised training for 3D morphable model regression," in *Proc. IEEE/CVF Conf. Comput. Vis. Pattern Recognit.*, Jun. 2018, pp. 8377–8386.
[179] S. Cheng, M. Bronstein, Y. Zhou, I. Kotsia, M. Pantic, and S. Zafeiriou, "MeshGAN: Non-linear 3D morphable models of faces," 2019, *arXiv:1903.10384*.
[180] S. Moschoglou, S. Ploumpis, M. A. Nicolaou, A. Papaioannou, and S. Zafeiriou, "3DFaceGAN: Adversarial nets for 3D face representation, generation, and translation," *Int. J. Comput. Vis.*, vol. 128, nos. 10–11, pp. 2534–2551, Nov. 2020.
[181] B. Gecer, S. Ploumpis, I. Kotsia, and S. Zafeiriou, "Fast-GANFIT: Generative adversarial network for high fidelity 3D face reconstruction," 2021, *arXiv:2105.07474*.
[182] A. Jain, D. Way, V. Gupta, Y. Gao, G. de Oliveira Marinho, J. Hartford, R. Sayres, K. Kanada, C. Eng, K. Nagpal, K. B. DeSalvo, G. S. Corrado, L. Peng, D. R. Webster, R. C. Dunn, D. Coz, S. J. Huang, Y. Liu, P. Bui, and Y. Liu, "Development and assessment of an artificial intelligence–based tool for skin condition diagnosis by primary care physicians and nurse practitioners in teledermatology practices," *J. Amer. Med. Assoc. Netw. Open*, vol. 4, no. 4, Apr. 2021, Art. no. e217249.

ANWESHA MOHANTY (Graduate Student Member, IEEE) was born in Bhubaneswar, India. She received the B.Tech. degree in computer science and engineering from the Biju Patnaik University of Technology, India, in 2014, and the M.Tech. degree in computer science and engineering from Christ University, Bengaluru, India, in 2017. She is currently pursuing the Ph.D. degree with the Centre for Research Training in Digitally-Enhanced Reality (d-real), School of Computing, Dublin City University, Dublin, Ireland.

Her key research interests include medical, clinical, and biological-image data analysis, with the application of image processing, computer vision, and machine learning.

Ms. Mohanty was a recipient of two years of Master's by Research Scholarship from the Faculty of Engineering and Computing, Dublin City University, and four years of Ph.D. Scholarship from the Science Foundation Ireland Centre for Research Training in DigitallyEnhanced Reality (d-real).

ALISTAIR SUTHERLAND received the bachelor's degree in physics from the University of Cambridge, in 1982, and the Ph.D. degree in image processing from The University of Edinburgh, in 1989. He was a Postdoctoral Researcher in statistical image analysis and machine learning at the University of Strathclyde and the University of Glasgow. He worked on sign language recognition at the Hitachi Dublin Laboratory, from 1993 to 1996. He spent 25 years as a Lecturer at the School of Computing, Dublin City University. His research interests include computer vision for human motion analysis for sign language recognition and a public speaking tutorial systems. He retired in 2021.

MARIJA BEZBRADICA received the B.Sc. and M.Sc. degrees in electrical engineering from the School of Electrical Engineering, University of Belgrade, Serbia, in 2007 and 2008, respectively, and the Ph.D. degree in complex systems modeling from Dublin City University (DCU), Ireland, in 2013, on building stochastic models for prediction of complex drug dissolution.

She was a Postdoctoral Research at DCU included application of similar predictive methods on understanding pedestrian behavior in large and complex urban networks. Her current research interests include interdisciplinary and inverse modeling methods, cellular automata and multi-agent systems, predictive and behavioral analytics in FinTech, bioinformatics and e-Health, applied mathematics, and high-performance computing.

HOSSEIN JAVIDNIA received the master's degree in computer network security from the University of Guilan, Iran, in 2015, and the Ph.D. degree in electronic and electrical engineering from the National University of Ireland Galway, in 2018, examining the contributions to the measurement of depth in consumer imaging.

He has experience as a Research and Development Engineer with Xperi Corporation, mainly focused on consumer 3D reconstruction. He also worked as a Postdoctoral Fellow with the ADAPT Centre, Trinity College Dublin, focused on advanced 3D modeling and augmented reality, a collaborative project with Huawei Ltd., Ireland, "Deep Real: Deep Learning for 3D Object placement in videos" nominated for Technology Award Ireland, in 2019. He is currently an Assistant Professor in software engineering with the School of Computing, Dublin City University.